CHAPTER 7 - WAVES AND TIDES

In this section we will explore unsteady open phenomena which are periodic. By unsteady we mean that $\frac{\partial}{\partial t} \neq 0$ as we assumed in the previous section. Thus the inertial acceleration will be important in addition to other terms in the momentum equation. By periodic we mean a characteristic parameter f of a process repeats itself in space over a scale L such that

$$f(x + L) = f(x),$$

or in time over an interval T such that

$$f(t + T) = f(t),$$

or both.

In general, waves result from disturbances to a mechanical system that is in static equilibrium. The restoring forces attempt to return the system to equilibrium, but overshoots occur and oscillations (i.e. waves) result.

In the ocean, winds are very often the agent that disturbs the sea surface of the ocean. (The gravitational effects of the moon and sun also disturb the sea surface.) As gravity attempts to restore the sea surface distortion to its equilibrium state, the potential energy of the original distortion is converted to kinetic energy in the velocity field and the lowering sea surface overshoots until the gravitational restoring force reverses the process. A surface gravity wave is generated and its energy propagates away from its generation site. Surface gravity waves are the result.

The wave spectrum in Figure 7.1 shows how surface wave energy is distributed among many wave frequencies in the ocean. Wind-driven surface gravity waves wind periods in the 1 to 30 second range are the most energetic, followed by tides. Note that short period (or high frequency) capillary wave motion is controlled by surface tension, while

longer period (or low frequency) gravity waves, like storm surges and tides, are also influenced by earth rotation.

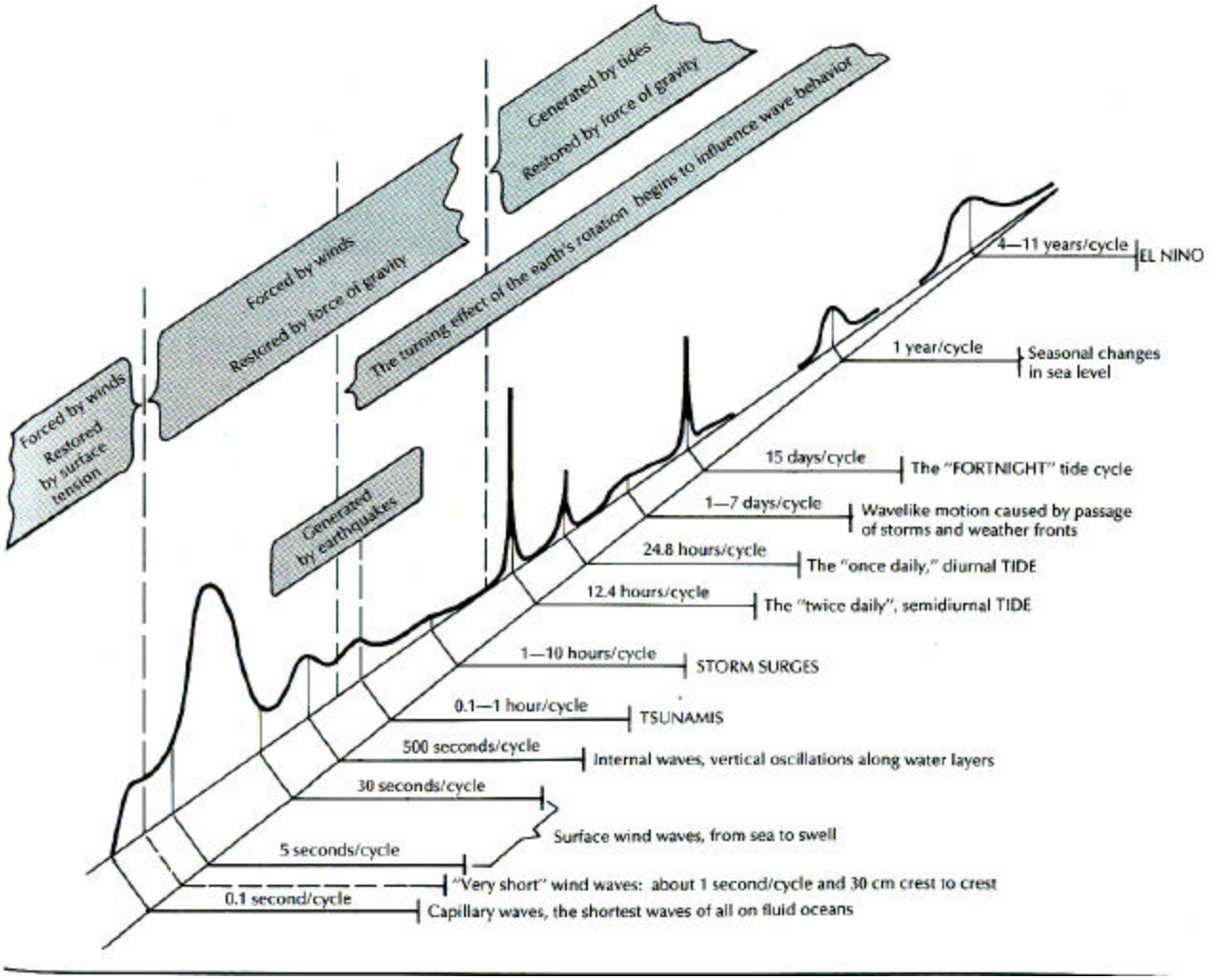

Figure 7.1. A spectrum diagram of how energy in the many different types of ocean waves is distributed according to frequency. Waves are identified according to wave period and to the disturbing and restoring forces which act at different time scales. (Neshyba 1987)

Surface Gravity Wave Model

Here we consider a simplified model for surface gravity waves. As we all have observed the sea surface at a particular location is a complicated superposition of waves with different characteristics propagating from different places where they were usually generated by the wind at different times. However, first we want to focus on the basic principles of wave motion, so we will explore a simple monochromatic (i.e. single frequency) wave model. Later we will apply this understanding of the "essential

physics" of wave motion toward more realistic observed wave fields.

To start, we define the characteristics of our monochromatic wave in terms of a sine wave which has been frozen in time and in space (see Figure 7.2). The definitions of terms are:

ELEVATION: $h(x,t)$ is the instantaneous vertical departure of sea level from the undisturbed sea level.

WAVE HEIGHT: H is the distance between the wave crest and trough.

AMPLITUDE: $a = \frac{1}{2} H$

WAVELENGTH: L the distance between points of equal phase.

WAVENUMBER: $k = \frac{2p}{L}$, the number of times a wave can fit on the circumference of circle with a dimensionless radius = 1.

$[k] = (\text{length})^{-1}$

WAVE PERIOD: T, is the time between points of equal phase.

[T] = unit time.

WAVE FREQUENCY: $f = \frac{1}{T}$ is the number of complete cycles per unit time.

$[f] = \frac{\text{cycles}}{\text{time}}$

ANGULAR FREQUENCY: $w = \frac{2p}{T} = 2p\, f$ is the number of times a wave of period T can fit on the circumference of a circle with a dimensionless radius = 1.

$[w] = (\text{time})^{-1}$

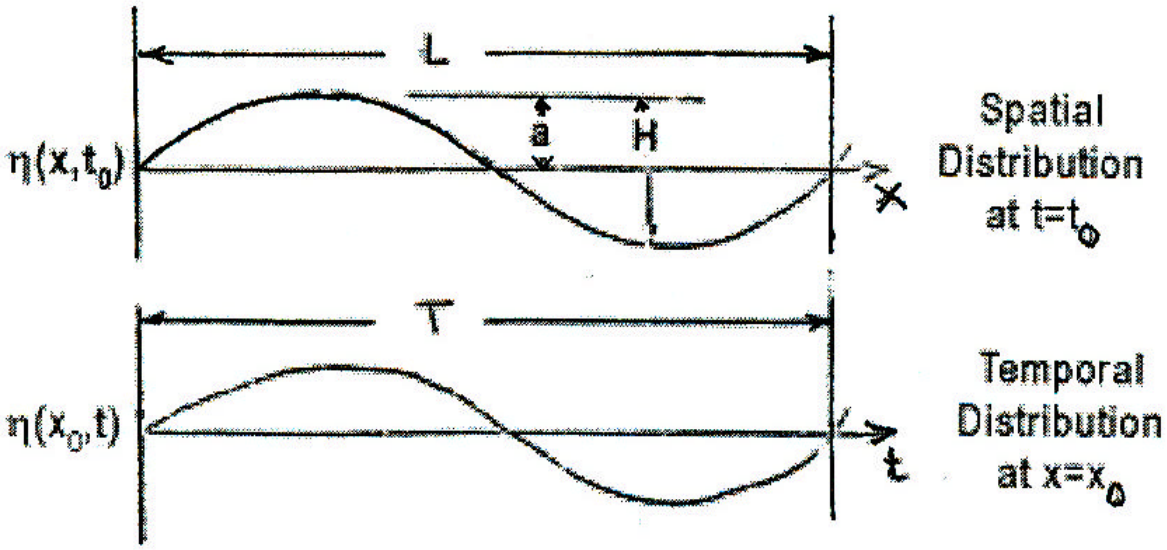

Figure 7.2. A monochromatic sine wave is (above) "frozen" in space and (below) measured at a fixed station

From these definitions, we define the speed of a particular point on a waveform (or the phase) as the phase speed, c where

$$c \equiv \frac{L}{T} \quad \underline{OR} \quad c \equiv \frac{w}{k}. \qquad [c] = \frac{\text{length}}{\text{time}}$$

This is a kinematical relationship and it is true for all waves.

The mathematical description of our monochromatic "right-traveling" waveform is

$$h(x, t) = a \cos\left(\frac{2p\ x}{L} - \frac{2p\ t}{T}\right)$$
$$= a \cos(kx - w t).$$

It can also be written in terms of phase speed as

$$h(x, t) = a \cos[k(x - ct)].$$

The part in parentheses above are different forms of what is called the *phase* of the

wave. If we ride with the wave (as surf riders do), then we are actually following a specified point on the waveform. Thus the phase of the wave appears to be constant to us surf riders and the following relation holds;

$$(\frac{2p\ x}{L} - \frac{2p\ t}{T}) = \text{constant}\ .$$

If we choose to follow the wave crest then by definition the constant = 0. What is the relation between x (our position in absolute space) and time? The answer is found by rewriting the constant phase relation above in terms of x as follows

$$x = \frac{L}{2p}(\frac{2p\ t}{T}) = \frac{L}{T}\ t$$

OR

$$x = ct$$

Thus it can be seen that we are moving with the phase speed c towards + x. Convince yourself that a left traveling wave (towards -x) is described according to

$$h = a\cos(\frac{2p\ x}{L} \underset{\text{NOTE}}{\uparrow} + \frac{2p\ t}{T})\ .$$

So far we have considered only the kinematics of the wave. To discover any relation between wave period T and wavelength L the dynamics must be considered. Here we will consider the model of *Airy Waves* in two dimensions.

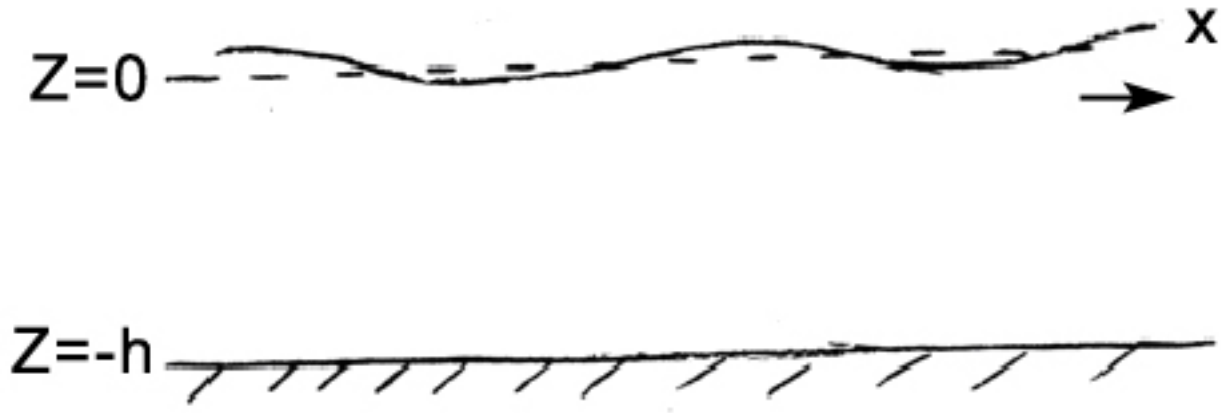

Figure 7.3. Airy wave model geometry.

The model geometry (Figure 7.3) and the following assumptions form the basis for solving the appropriate momentum equations.

Assumptions:

(1) a << L and a << h
(This means that surface wave form slopes (i.e. a/L) are small and the non-linear acceleration terms (i.e. $(\vec{V} \bullet \nabla)\vec{V}$ terms) can be neglected).

(2) Uniform depth
(h = constant)

(3) A non-viscous and irrotational ocean.
(This means that the vorticity is zero).

(4) Fluid is incompressible and homogeneous
Thus acoustic and internal waves (due to density stratification) are not present.

(5) Earth rotation is unimportant
(Thus Coriolis effects are negligible and very long period waves are excluded).

(6) No surface tension.
(This condition excludes capillary waves and other very short waves).

(7) A smooth and impermeable bottom.

(8) Uniform atmospheric pressure.

(9) Two-dimensional - i.e. no y variations.

The implications of these different assumptions are as follows:

A. No vorticity in (3) means that in two dimensions

$$\frac{\partial u}{\partial z} - \frac{\partial w}{\partial x} \equiv 0$$

B. The 2-D continuity relation reduces to

$$\frac{\partial u}{\partial x} + \frac{\partial w}{\partial z} = 0 .$$

C. The x and z momentum equations become

$$\frac{\partial u}{\partial t} = - \frac{1}{r} \frac{\partial r}{\partial x}$$

and

$$\frac{\partial w}{\partial t} = - \frac{1}{r} \frac{\partial p}{\partial z} - g ,$$

respectively.

The vertical momentum equation describes the balance between vertical acceleration, the gravitational restoring force, and the pressure gradient force which helps to convert vertical motion into horizontal motion. That can be seen in the horizontal momentum equation which converts horizontal pressure gradient forces into horizontal accelerations. The above relationships above must be satisfied at all times everywhere in the domain of interest!

In principle, the following conditions at the upper and lower boundaries

(i.e. *boundary conditions*) must be satisfied for all times;

(a) at $z = h$ $\quad w = \frac{\partial h}{\partial t}$

(b) at $z = h$ $\quad p = 0$

© at $z = -h$ $\quad w = 0$

However, for small ? the following *approximate boundary conditions* can be used instead;

At z = 0 $w = \frac{\partial h}{\partial t}$ and p = ρ g?

At z = -h w = 0

For an assumed waveform ? = a cos(kx - ω t), *the solution* to the approximate equations of motion and boundary conditions above is

$$u = a\omega \frac{\cosh k(z+h)}{\sinh (kh)} \cos(kx - \omega t)$$

$$w = a\omega \frac{\sinh k(z+h)}{\sinh (kh)} \sin(kx - \omega t)$$

$$p = -\rho gz + \rho ga \frac{\cosh k(z+h)}{\cosh kh} \cos(kw - \omega t)$$

plus the *dispersion relation*

$$\omega^2 = gk \tanh(kh),$$

which describes the relation between wave frequency and wave number. Note that this solution is given in terms of *hyperbolic functions*. These may be new to some people so they are briefly discussed next.

Digression

---

tan(kh) is the hyperbolic tangent of kh. The hyperbolic tangent of x is defined as

$$\tanh(x) = \frac{\sinh(x)}{\cosh(x)} = \frac{\frac{e^x - e^{-x}}{2}}{\frac{e^x + e^{-x}}{2}} = \frac{e^x - e^{-x}}{e^x + e^{-x}} \quad ,$$

where

$$\frac{d}{dx}[\cosh(x)] = \sinh(x)$$

and

$$\frac{d}{dx}[\sinh(x)] = \cosh(x) .$$

See Figure 7.4 for graphical descriptions

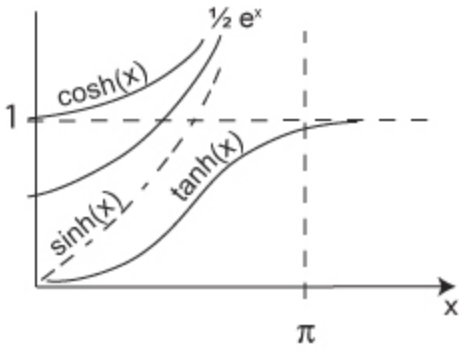

Figure 7.4 Plot of hyperbolic sine, cosine, and tangent of x and their dependences on x. in our application x=kh.

.

The *dispersion relation* given above can be rewritten as

$$c^2 = \frac{L^2}{T^2} = \frac{w^2}{k^2} = \frac{g}{k}\tanh(kh) \ ,$$

which shows that, in general, Airy waves have phase speeds which depend upon wave number k (or wavelength L) (see Figure 7.5).

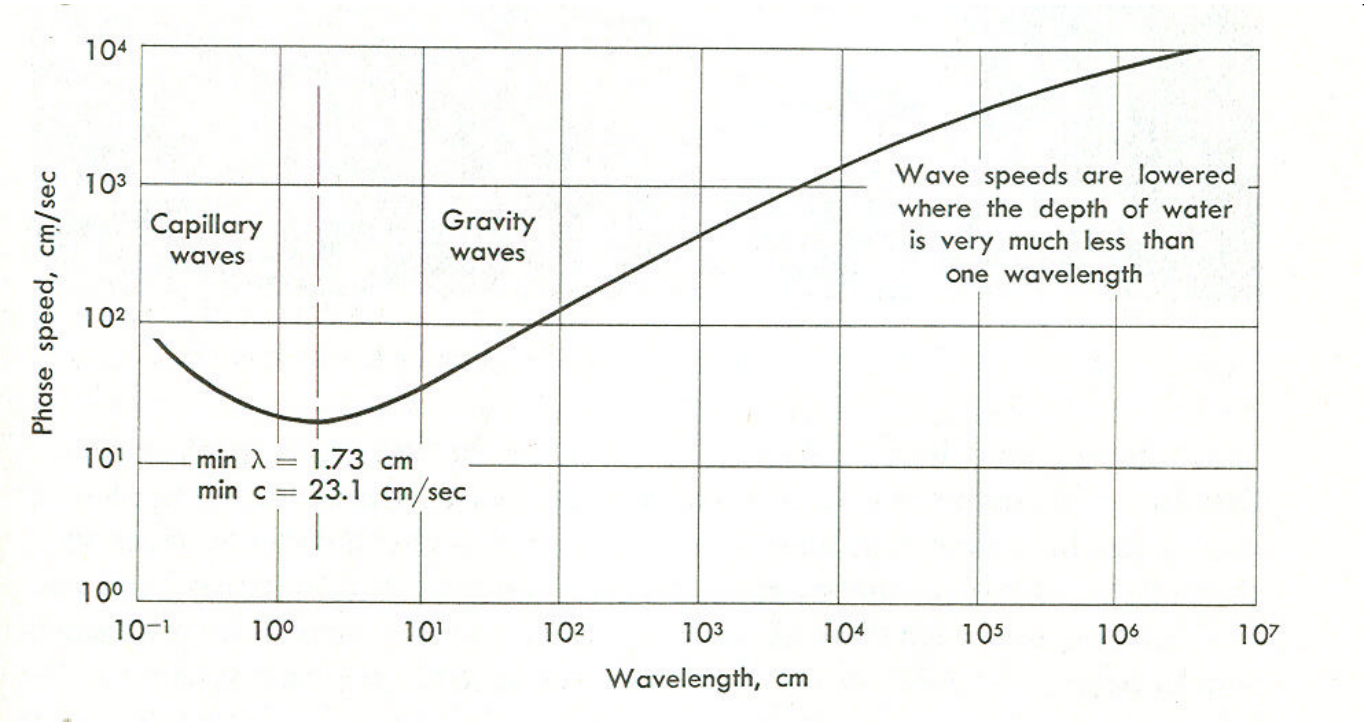

Figure 7.5. The celerity or phase speed of gravity waves and capillary waves as a function of their wave length. (von Arx, 1974)

Two important approximations to the wave solutions above yield short and long wave length limits.

Short waves have wavelengths that are much less than the water depth so they are "deep water waves". Mathematically this means that kh is large, i.e. $kh > p$ or $\frac{2p\,h}{L} > p$, which means that the depth of the water is greater than ½ the wavelength or $h > L/2$.

Thus the dispersion relation for *short wave* (deep water waves) becomes

$$c^2 = \frac{w^2}{k^2} = \frac{g}{k} = g\frac{L}{2p} \quad ,$$

which reduces to

$$c = \sqrt{\frac{1}{2p}(gL)}$$

Since L = c x T, the above can also be written

$$c = \frac{1}{2p}(gT) .$$

For large kh, sinh(kh) and cosh(kh) both become $\frac{e^{kh}}{2}$ (see Figure 7.4 above), the *short wave solutions* become

$$h = a \cos(kx - w t)$$
$$u = a w e^{kz} \cos(kx - w t)$$
$$w = a w e^{kz} \sin(kx - w t)$$
$$p = r g a e^{kz} \cos(kx - w t) - r gz$$

The wave kinematics are shown schematically in Figure 7.6 for different water depths. Note the relative phases of h , u, w and p fields.

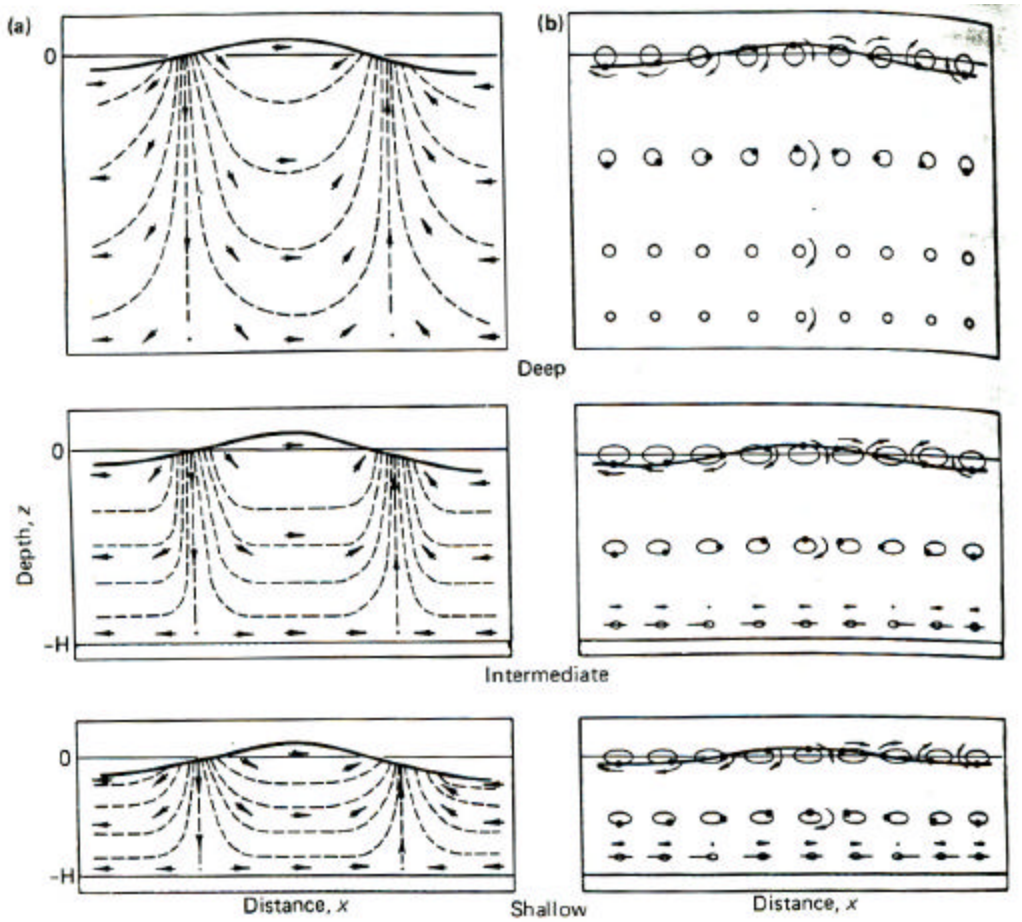

Figure 7.6. Kinematics of waves propagating left to right in (top) deep water; (middle) intermediate depth water; (bottom) shallow water. The left panels (a) are instantaneous snapshots of the water parcel streamlines. The right panels (b) show the trajectories of selected water parcels over a full wave cycle. (Knauss,1976; after Kinsman in Water Waves)

The motions associated with short or deep water waves decreases with depth, such that amplitudes at a depth of z = -L/2 are e^{-p} or 4% of surface values. This can be seen in the water parcel trajectories as the wave passes in Figure 7.7.

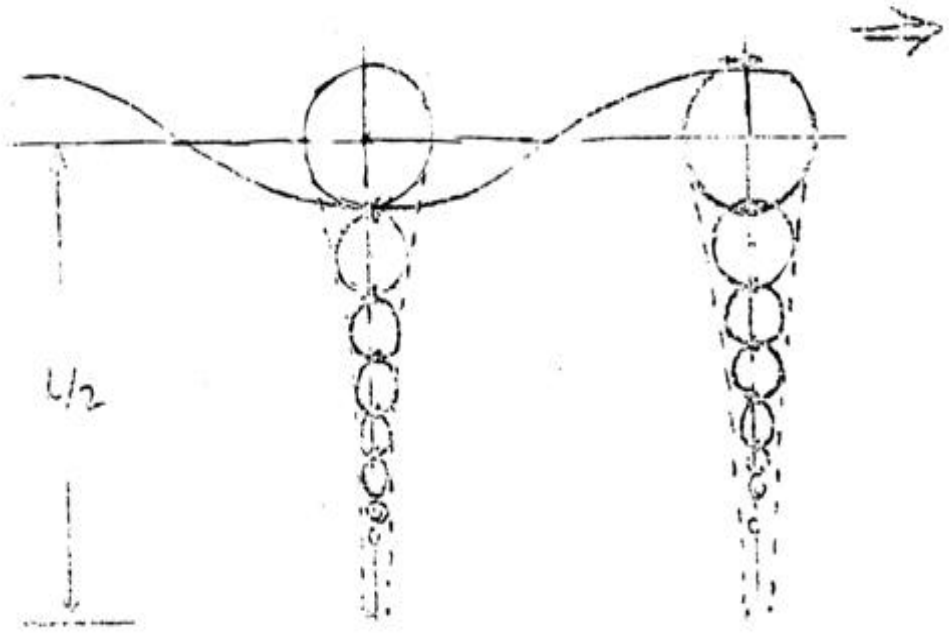

Figure 7.7 Deep water Airy wave parcel orbital diameters decay exponentially to about 4% of the surface over a depth h= – z = L/2 - a half wave length.

For *long waves*, the wavelength is much greater than the water depth, so long waves "feel the bottom" and are called *shallow water waves*.

Mathematically, this means that

$$kh < \frac{p}{10} \text{ or } h < \frac{1}{20} L .$$

For small kh

$$\tanh(kh) \sim kh$$

and the *long wave* dispersion relation becomes

$$c^2 = \frac{w^2}{k^2} = \frac{g}{k} kh$$

so that

$$c = \sqrt{gh}$$

Long (or shallow water) waves are *non-dispersive*, that is that their speed is independent of wavelength. This is demonstrated in the in Figure 7.8 which depicts the relation of wave phase speed and wavelength for different water depths.

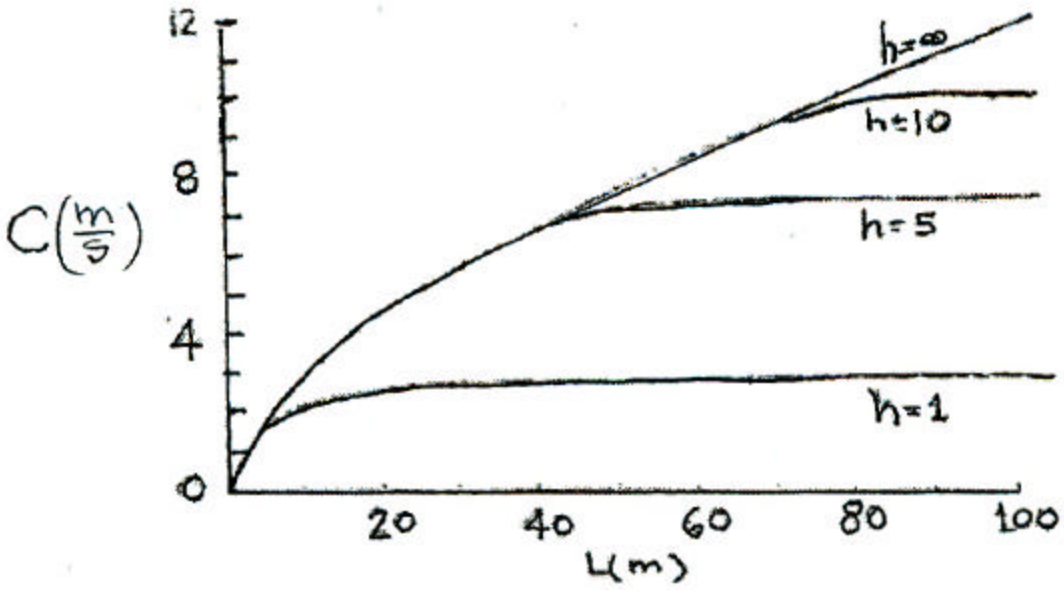

Figure 7.8 Wave phase speed versus wave length L(m) – a dispersion diagram for Airy waves in different water depths h(m).

Figure 7.9 shows water parcel orbits during the passage of a *long (or shallow) water wave* in very shallow water. Notice that most of the motion is horizontal, much like what scuba divers feel in shallow water with a long swell.

Figure 7.9. Wave water parcel orbital paths in very shallow water.

For shallow water waves pressure and horizontal velocity are undiminished with depth.

Wave Energy

Of course in the real ocean the surface is composed of more that one monochromatic wave. What are the consequences? To answer the question, we increase the complexity of our model slightly by superposing two Airy waves with the same amplitude but slightly different frequencies and wave numbers such that $w_2 > w_1$ and $k_2 > k_1$. The resultant wave field is described by

$$h = \frac{a}{2}\cos(k_1 x - w_1 t) + \frac{a}{2}\cos(k_2 x - w_2 t)$$

which can be rewritten as

$$= \cos\left[\left(\frac{k_2 - k_1}{2}\right)x - \left(\frac{w_2 - w_1}{2}\right)t\right]\cos\left[\left(\frac{k_1 + k_2}{2}\right)x - \left(\frac{w_1 + w_2}{2}\right)t\right]$$

$$= \cos\left[\left(\frac{k_2 - k_1}{2}\right)\left(x - \frac{w_2 - w_1}{k_2 - k_1}t\right)\right]\cos\left[\left(\frac{k_1 + k_2}{2}\right)\left(x - \left(\frac{w_1 + w_2}{2}\right)t\right)\right]$$

This can be simplified by recognizing that the cos[ ] to the right in the relation above represents a wave with intermediate frequency and wavelength and therefore is nearly indistinguishable from the parent waves. On the other hand, the cos[ ] on the left

represents a wave with much greater L (smaller k) traveling at a speed

$\frac{\Delta w}{\Delta k} = \frac{w_2 - w_1}{k_2 - k_1} = c_g$, which we called the *group speed*.

Thus the amplitude of the resultant wave is modulated according to:

$$h = a\cos\left[\frac{\Delta k}{2}(x - c_g t)\right]\cos\left[\bar{k}(x - \bar{c}t)\right] \quad ,$$

where

$$\bar{k} = \frac{k_1 + k_2}{2}\,;\ \bar{c} = \frac{\bar{w}}{\bar{k}}\,;\ \text{and}\ \bar{w} = \frac{w_1 + w_2}{2}\ .$$

and is shown in Figure 7.10.

Figure 7.10. Wave envelope of a pair of interfering deepwater surface gravity waves.

The packets of waves that result from the superposition are known as *wave groups* and $c_g = \frac{dw}{dk}$ is shown as the *group velocity.* The group velocity for Airy waves is

$$c_g = \frac{dw}{dk} = \frac{d}{dk}\left[gk\tanh(kh)\right]^{1/2}$$

$$c_g = \frac{1}{2}c\left(1 + \frac{2kh}{\sinh 2kh}\right)$$

which for <u>long waves</u> (small kh)

$c_g = c$ *shallow water waves*

and for <u>short waves</u> (large kh)

$$c_g = \frac{1}{2} c \qquad \textit{deep water waves}$$

The group velocity is the velocity at which *wave energy* is transmitted. Wave energy is composed of both the kinetic and potential energy components which can be computed for Airy waves.

In general the average kinetic energy per unit surface area for a wave can be expressed as

$$\overline{KE} = \frac{1/2\ r}{L} \int_0^L \int_{-h}^{h} (u^2 + w^2)\, dxdz$$

and the wave potential energy can be found by computing first the total potential energy for the waveform (Figure 7.11).

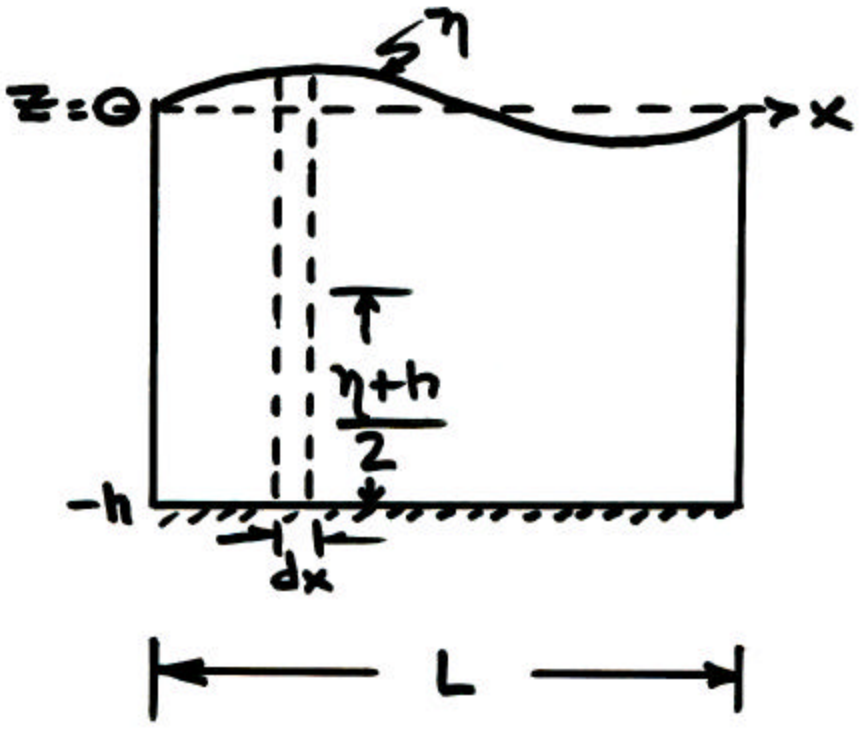

Figure 7.11 Diagram for computing wave potential energy.

The total potential energy of a wave per unit width is

$$PE = \int_0^L [\rho g(? + h)][(? + h)/2]\, dx$$

so that

$$PE = \int_0^L \rho g \frac{(? + h)^2}{2}\, dx = \underbrace{\rho g \frac{h^2 L}{2}}_{(a)} + \int_0^L \underbrace{\rho g[\frac{h^2}{2} + \underbrace{h}_{(b)} h]}_{(c)}\, dx$$

Term (a) is the potential energy of the "still water" and therefore is not available for wave motion.

Term (c) is <u>zero</u> when averaged over a wave length of a periodic wave.

Therefore the average wave potential energy per unit surface area, $\overline{PE} = PE/L$, is

$$\overline{PE} = \frac{\rho g}{2L} \int_0^L h^2\, dx ,$$

which upon substitution of the actual waveform $h = a \cos \frac{2\pi x}{L}$. reduces to

$$\overline{PE} = \frac{1}{2} \frac{\rho g a^2}{L} \int_0^L (\cos^2 kx)\, dx = \frac{1}{2} \frac{\rho g a^2}{L} \int_0^L \left[\frac{(1 + \cos 2kx)}{2} \right] dx \quad .$$

Performing the final integration gives

$$\overline{\overline{PE} = \frac{1}{4} \rho g a^2 .}$$

The average kinetic energy for the wave $\overline{KE}$ can be computed using the Airy wave solutions for velocity in the general relation above. Since ? is small we can assume ? ~ 0 with negligible error and integrate leading to

$$\overline{KE} = \frac{1}{4} \rho \frac{(a\omega)^2}{k} \coth(kh)$$

But since $\omega^2 = gk \tanh(kh)$ or $\frac{k}{\coth(kh)} = \frac{\omega^2}{g}$, the average wave kinetic energy per unit surface area is

$$\overline{KE} = \frac{1}{4} \rho g a^2 = \overline{PE}$$

For Airy waves there is *equipartition of energy between kinetic and potential energy*. The *total average wave energy* per unit surface area is then

$$\overline{E} = \overline{PE} + \overline{KE} = \frac{1}{2} \rho g a^2$$

In terms of wave height, which is easier to estimate, this becomes

$$\overline{E} = \frac{1}{8} \rho g H^2$$

From the expression for $\overline{E}$ we can compute the wave power per unit length of wave front according to

$$\overline{P} = \overline{E} c_g$$

where c_g in the wave group velocity.

For Airy waves in deep water the group velocity is

$$c_g = \frac{1}{2} c = \frac{1}{2} \sqrt{\frac{1}{2p} (gL)}$$

or

$$= \frac{1}{2} (\frac{1}{2p} gT) = \frac{1}{4p} gT \ .$$

which again is more easily estimated for the latter form. Thus

$$\overline{P = \frac{1}{32p} r \, g^2 TH^2}$$

For Airy waves in shallow water

$$c_g = \sqrt{gh} \quad \text{and}$$

$$\overline{P = \frac{1}{8} r \, g H^2 \sqrt{gh}}$$

History of a Wind-Driven Wave

Let us now explore a brief history of real group of surface waves generated by a storm at sea. The basic assumption here is that the superposition of a group of Airy waves with different characteristics approximates the real sea surface. We will now consider the amount of wave energy in a frequency bandwidth from $w_o - \frac{1}{2} dw$ to $w_o + \frac{1}{2} dw$

shown schematically in Figure 7.12.

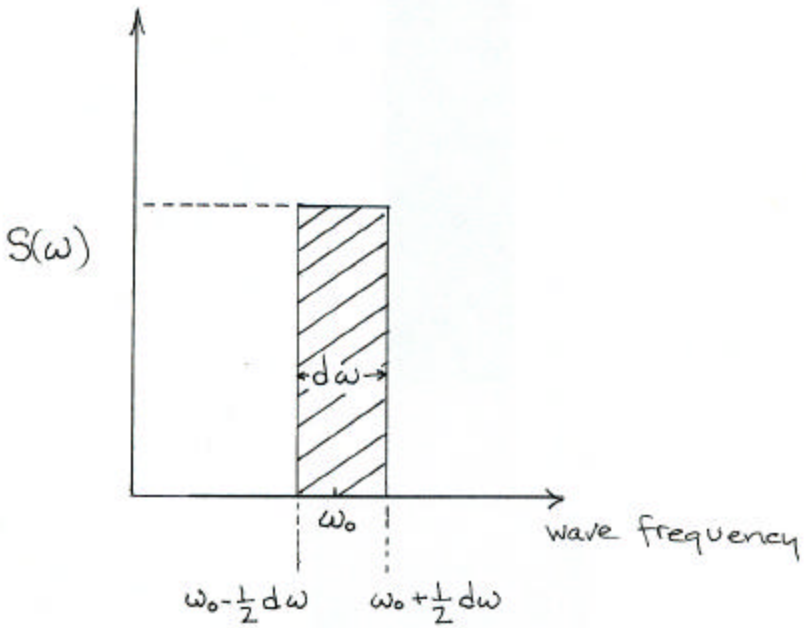

Figure 7.12. Spectral energy density diagram, showing the amount of wave energy in a frequency band dw centered on w_o

The energy in the cross-hatched area in Figure 7.12 is defined as mean squared ?(?) or

$$\overline{h^2} = \frac{1}{2r}\int_0^{2p} h^2 \, \mathrm{d}(w\,t) = \frac{a^2}{2} \qquad ,$$

where ? = a cos(? t). Note that $\overline{h^2}$ is proportional to $\overline{E} = \frac{1}{2}\, r\, g\, a^2$ and is related to S(w), the energy density or energy per unit bandwidth according to

$$S(w)\, dw = \frac{a^2}{2}.$$

An energy density spectrum, which describes energy distribution at all frequencies, can be constructed (e.g. Figure 7.13). A suite of energy density spectra (Figure 7.13) and wave energy periodograms (Figure 7.14) for a fully developed sea for different wind speeds shown that higher winds generate more lower frequency waves.

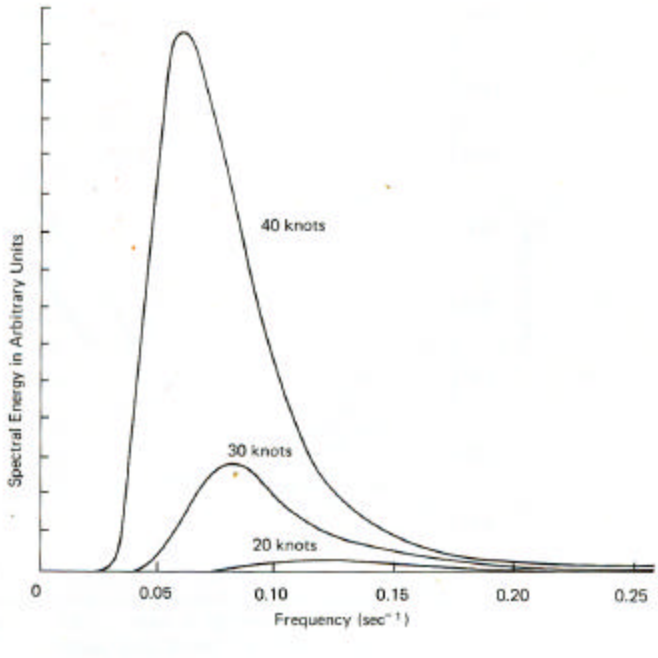

Figure 7.13. *Energy density spectra* of wind driven waves at different wind speeds. Note how the larger wind speeds generate waves for which the energy density peak migrates to lower frequencies. (Knauss, 1976)

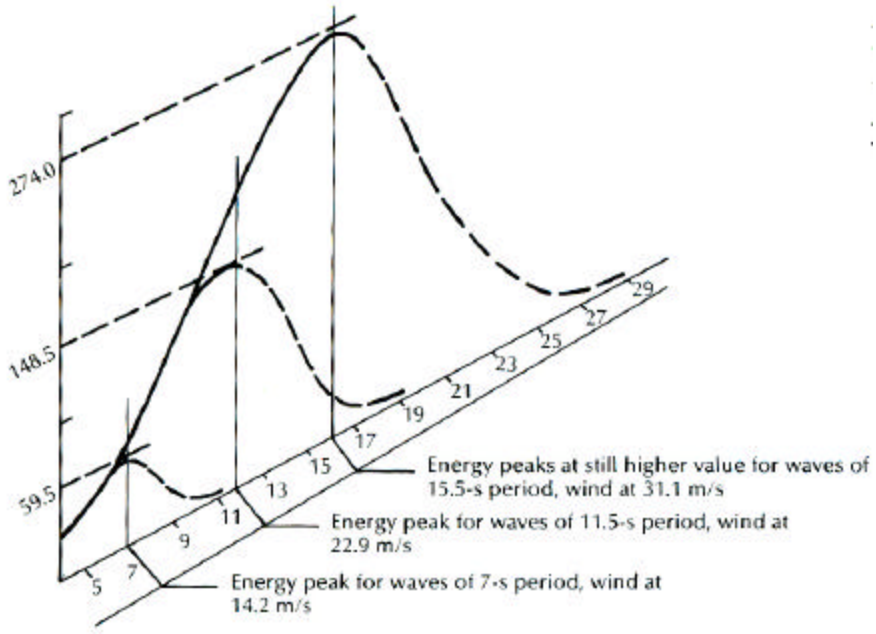

Figure 7.14 *Wave energy* (kilojoules/m^2) *periodogram* for wave fields generated by different wind speeds. (see Table 7.1 data; from Neshyba, 1987)

Table 7.1 Characteristics of wind waves observed at sea under different wind conditions (from Cornish 1934).

Wind Speed m/s	Wave Speed m/s	Period, T, seconds	Length, L, meters	Height, H, meters	H/L	Energy, kilojoules/m^2
14.2	11.5	7.0	78	6.9	0.088	59.5
16.0	12.8	8.0	103	7.7	0.074	74.1
19.2	16.3	9.5	147	9.2	0.063	106.0
22.9	18.3	11.5	209	10.9	0.052	148.5
27.0	21.5	13.5	290	13.0	0.045	211.0
31.1	25.0	15.5	384	14.8	0.039	274.0

Figure 7.14 summarizes the frequency distribution of the quantity $a^2/2$ which is proportional to wave energy.

After the wind stops blowing or the storm moves from the area of immediate wave generation, the waves with different period and thus different wavelengths will propagate at different speeds as indicated in Figure 7.15.

Figure 7.15. Wave dispersion separates waves generated in the wave generation region.

Remember that the longer wave groups are moving faster. The implication of this wave dispersion is that wave energy frequency spectra measured at the distant shore will differ from the wind-driven wave energy spectrum at the generation site (Figure 7.15) and furthermore will change with time as the slower wave groups arrive. An example of a set of such spectra one might measure in the "deep" water somewhat offshore from the coast.

Notice in Figure 7.16 how the wave energy at the lower frequencies (longer periods

and wavelengths) arrives earliest, followed on successive days by higher frequency wave energy (shorter periods and wavelengths) with its correspondingly lower energy.

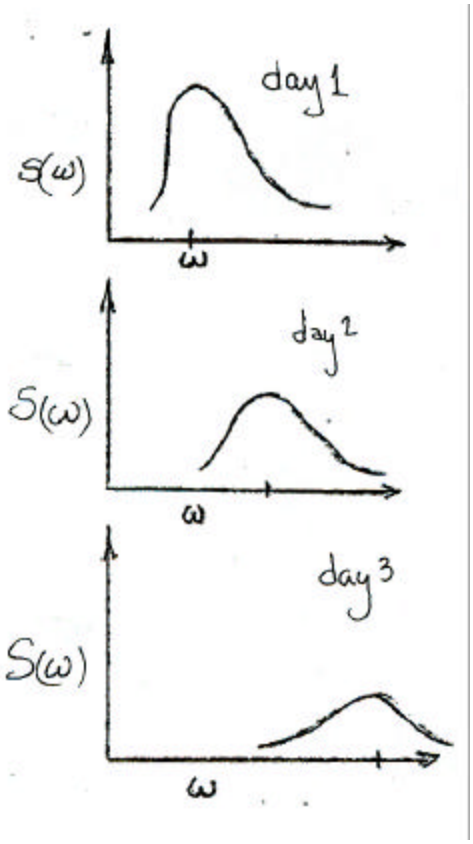

Figure 7.16. Wave energy density spectra for waves observed at a particular site on three successive days.

Eventually all of these wave propagate into water depths where they will become shallow water waves and therefore non-dispersive (refer to Figure 7.17).

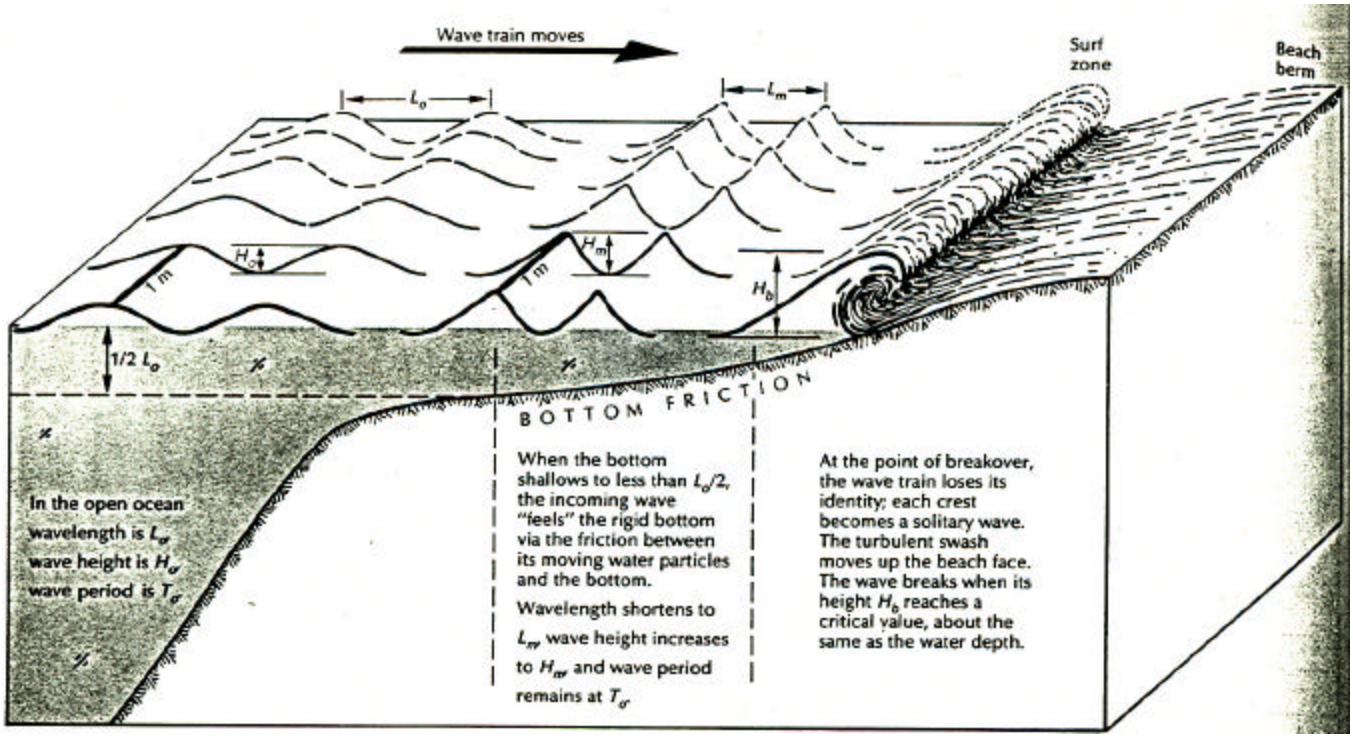

Figure 7.17. How a wave train is modified as it progresses from the open ocean toward the beach. In the open ocean the wave feels no frictional contact with the bottom. Once frictional contact begins, the wave changes in several ways simultaneously; the wave's speed drops, its height increases, and its direction shoreward becomes more and more perpendicular to the beach line. (Neshyba, 1987)

The phase speed and the group speed both are related to the water depth which decreases shoreward. Thus

$$c = c_g = \frac{L}{T} = \sqrt{gh}$$

and the wave period, T, can be expressed as

$$T = \frac{L}{\sqrt{gh}}$$

Since the number of waves are conserved as the wave train propagates shoreward, the wave period remains constant (i.e., T = constant). Thus L must decrease in proportion to $\sqrt{gh}$. The average wave power (per unit length of wave front) is

$$\overline{P} = \frac{1}{8}\, r\, g\, H^2\, c_g = \frac{1}{8}\, r\, g\, H^2 \sqrt{gh}$$

and along a straight beach with uniform bottom contours this must remain constant. Therefore, since

$$H^2 = \left(\frac{8\overline{P}}{r\, g^{3/2}} \right) h^{-1/2},$$

H must also increase!

As a result the wave slope which is proportional to H/L will increase to the point where Airy wave theory no longer applies. Continued increase of wave slope, which is indicated by further shoreward progress, will eventually lead to significant non-linearities and *wave-breaking*.

Before breaking the interaction of shoaling waves and the bottom lead to wave front bending or wave refraction. The sketch below shows how the upper left hand portion of the impinging wave front "feels" the bottom first and therefore slows relative to the lower right hand portion which still resides in deeper water.

The consequences of wave refraction near irregular coastlines is shown for two examples below. Each show how wave crests are refracted by the bathymetry. Thus the ray paths, which indicated the direction of wave energy propagation, are also distorted. In the case of a "point of land" (Figure 7.18) the equidistant rays in deep water are seen to converge on the point thereby concentrating wave energy there relative to other parts of the coastline. The opposite is true for a bay.

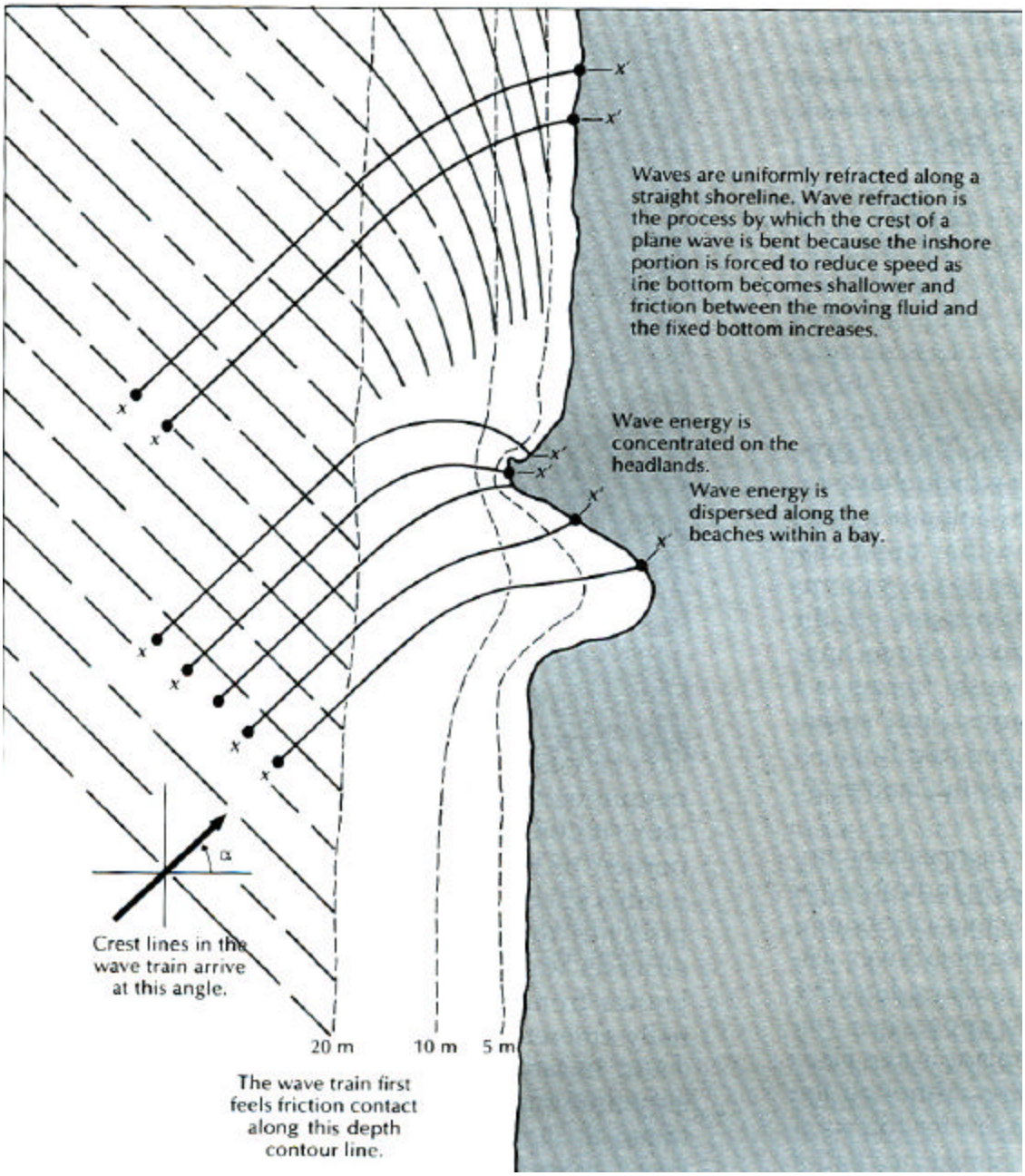

Figure 7.18 Wave refraction upon shoaling (above); concentration of energy on "points" (below). (Neshyba, 1987)

Standing Waves and Wave Reflection

Waves propagate toward shallower water, where they encounter shoaling water. It is not unusual that the wavelength L of the incident wave is much larger than the characteristic horizontal distance x_o of the encountered bottom slope (see Figure 7.19). Under these circumstances, the slope appears like a vertical wall to the wave and wave

reflection is probable. In general the reflected wave amplitude is usually smaller than that of the incident wave. However a superposition of an incoming or incident wave and an outgoing or reflected wave can lead to a standing wave pattern.

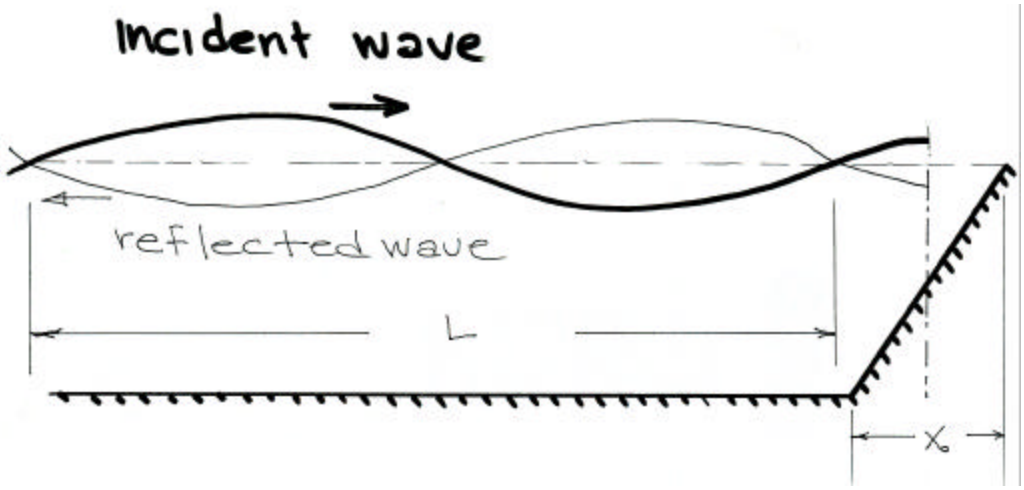

Figure 7.19 Propagation of a long wave into shoaling water.

The consequences of such a wave superposition can be seen by adding a rightward-propagating incident wave to a leftward-propagating reflected wave of equal amplitude according to:

$$h = \frac{a}{2}\cos(kx - \omega t) + \frac{a}{2}\cos(kx + \omega t)$$

$$h = a\cos(2\pi \frac{x}{L})\cos(\frac{2\pi}{T} t).$$

The resulting waveform is a non-propagating or <u>standing wave</u> (Figure 7.20) for which there is no vertical oscillation at its <u>nodes,</u> located at $x = n L/4$; for n = 1,3,5 ... odd integers. The maximum vertical motion in a standing wave takes place at the <u>anti-nodes,</u> located at $x = n L/4$ for n = 0,2,4 ...

even integers.

Since there is no horizontal motion (i.e. u =0) at the anti-nodes (as we will show below), vertical walls at such locations (e.g. x = L/2) without loss of generality. Exploring the relation between ? and u, as follows:

- at t = 0, T/2 and T, we find either maximum or minimum amplitude and

zero current everywhere.

- at t = T/4 or 3T/4, we find zero amplitude and either maximum current u or minimum current –u everywhere.

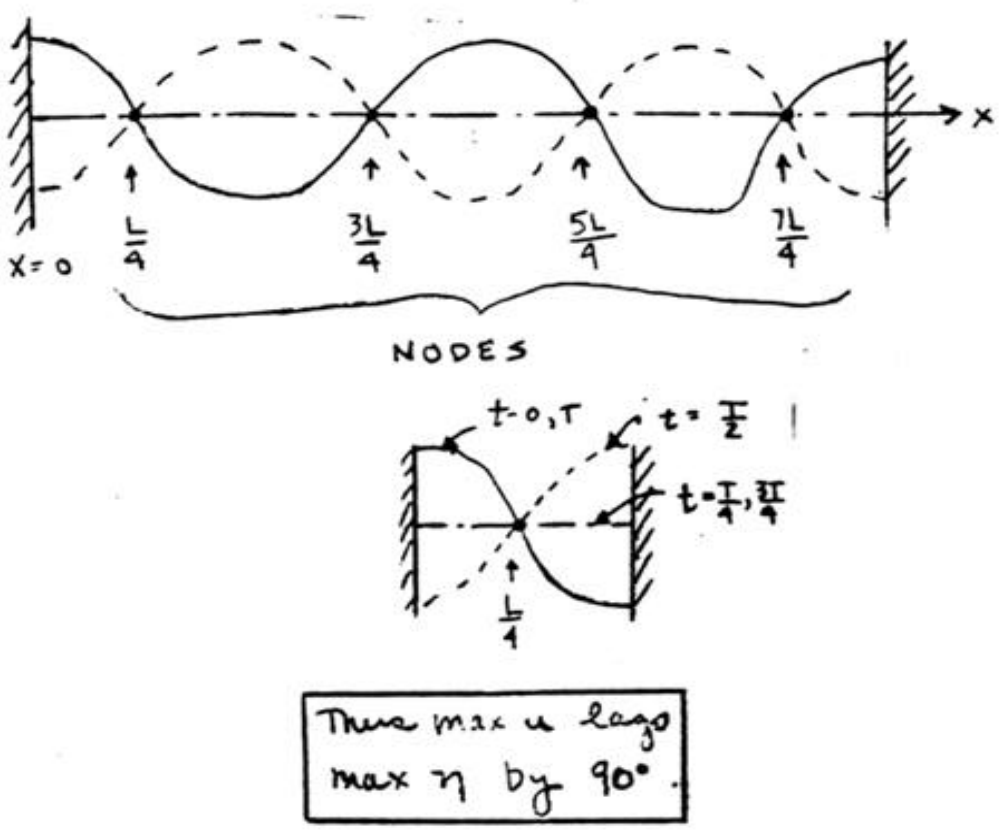

Figure 7.20. A standing wave pattern confined between a pair of vertical walls.

SEICHES: A Simple Case of Standing Shallow Water Waves

Consider the case of standing waves in an enclosed shallow water basin with a width W and constant depth = h; thus a fixed wave phase speed $c = \sqrt{gh}$. Also the standing wave anti-nodes must be located at the basin boundaries (Figure 7.21), because the horizontal current must be zero there.

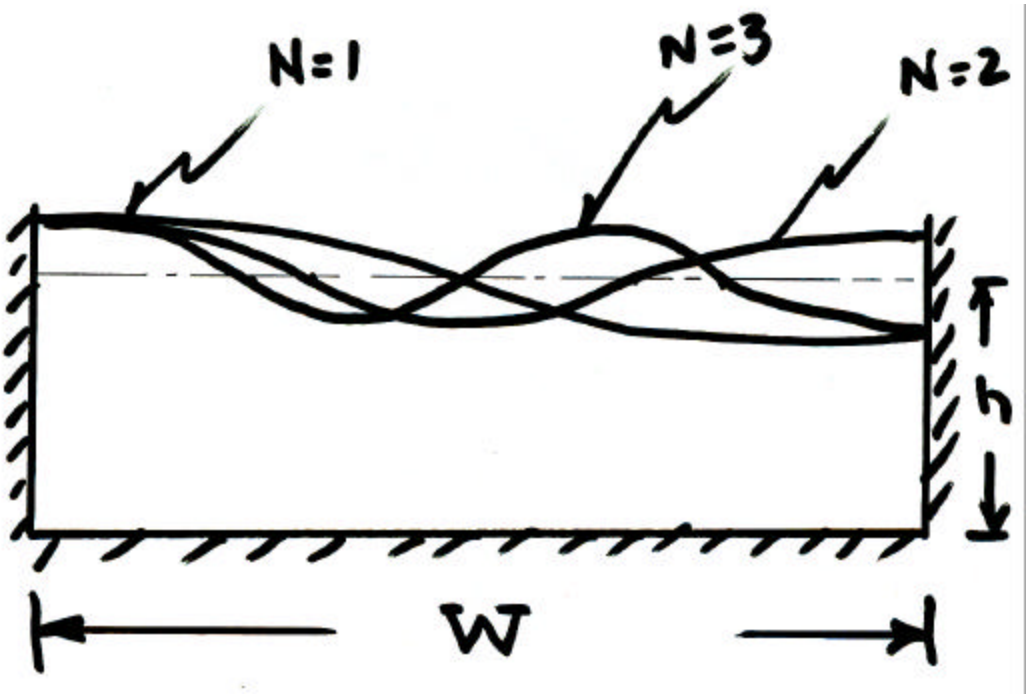

Figure 7.21 Different seiche modes in a shallow water basin.

This limits the possible half wavelengths of standing waves in the basin to submultiples of the basin length W, such that

$$L = \frac{2W}{1}, \frac{2W}{2}, \frac{2W}{3} .... \frac{2W}{N},$$

where N (= 1,2,3..positive integers) are the number of half waves contained in the basin. But, because $c = L/T = \sqrt{gh}$ = constant; or $L = T\sqrt{gh}$, substitution into rearrangement of the above relation shows that only certain wave frequencies are permitted, according to

$$f_N = \frac{1}{T_N} = \frac{\sqrt{gh}}{2W} N \qquad .$$

These f_N are the "natural oscillation" frequencies of the basin and are known as the basin *seiche frequencies*.

Long Wave Dynamics

The continuity relation for one-dimensional "long" waves $h\,(x,t)$ (propagating in a constant depth = h ocean for which $h/h \langle\langle 1$ is

$$\frac{\partial h}{\partial t} + h\,\frac{\partial u}{\partial x} = 0 \qquad \text{(a)}$$

where u is the vertically averaged horizontal velocity,

The appropriate momentum equation with bottom friction only is

$$\frac{\partial u}{\partial t} + u\,\frac{\partial u}{\partial x} = -\,g\,\frac{\partial h}{\partial x} - \frac{t_b}{h} \quad ,$$

where t_b is the bottom friction. The above relation can be further simplified by assuming linear and frictionless dynamics. Thus the momentum equation above becomes

$$\frac{\partial u}{\partial t} + g\,\frac{\partial h}{\partial x} = 0 \quad , \qquad \text{(b)}$$

which is a balance between the pressure gradient, due to sea surface tilt, and the inertial acceleration. By *operating on* the continuity relation [eq.(a)] with $\partial/\partial t$ and the momentum relation [eq.(b)] with $-\,h\,\partial/\partial x$, equations (a) and (b) become

$$\frac{\partial^2 h}{\partial t^2} + h\,\frac{\partial^2 u}{\partial t\,\partial x} = 0$$

$$+ -\,h\,\frac{\partial^2 u}{\partial t\,\partial x} - gh\,\frac{\partial^2 h}{\partial x^2} = 0 \quad .$$

respectively. Adding the two equations above, yields the following wave equation for ? alone

$$\frac{\partial^2 h}{\partial t^2} - gh\,\frac{\partial^2 h}{\partial x^2} = 0 \quad .$$

This is known as the Shallow Water or Long Wave Equation.

Application of the Shallow Water Wave Equation to the Coastal Ocean

Consider the one-dimensional, constant-depth, frictionless, continental shelf region (Figure 7.22), with a zero horizontal velocity (u = 0) boundary condition at the coast (at x = 0).

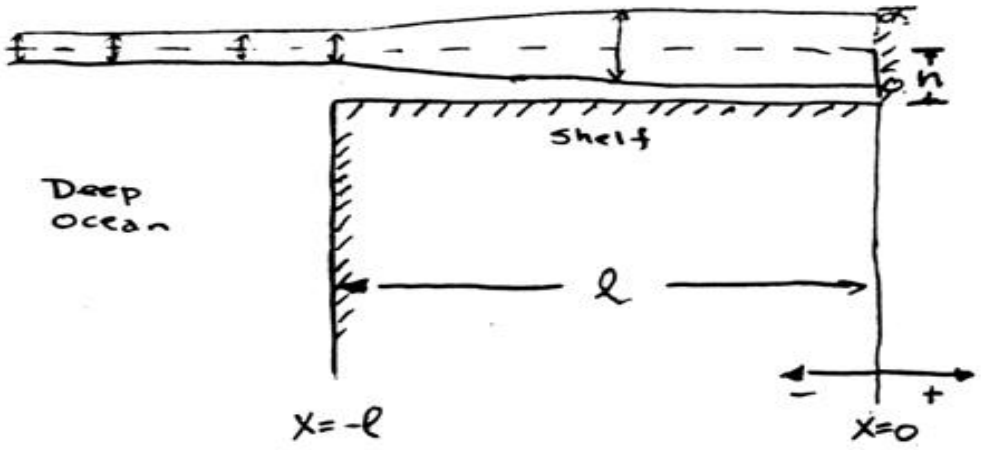

Figure 7.22 Standing shallow water waves over a continental shelf which results from an incident deep ocean wave with amplitude a_o.

The solution for shallow water waves on the shelf is composed of the sum of a right-hand propagating wave, with an arbitrary amplitude **a**, is

$$h^{+} = \frac{a}{2}\cos(kx - \omega t)$$

and a reflected left-hand propagating wave

$$h^{-} = \frac{a}{2}\cos(kx + \omega t) \quad ,$$

both with the dispersion relation

$$k = \frac{\omega}{\sqrt{gh}} .$$

The total wave solution on the shelf, which satisfies the continuity and momentum equations, and the velocity boundary condition at x = 0, is

$$h = h^{+} + h^{-} = a \cos(kx) \cos(w t) \quad ,$$

in which **a** is arbitrary wave amplitude to be determined. . To show the latter, use the continuity relation to find u from ? as follows:

$$-h \frac{\partial u}{\partial x} = + \frac{\partial h}{\partial t}$$

$$-h \frac{\partial u}{\partial x} = -w a \sin w t \cos kx \quad ,$$

which upon integration yields

$$u = \frac{w a}{kh} \sin kx \sin w t \quad ,$$

since $\frac{w}{k} = \sqrt{gh}$ = constant .

There are several features of this solution that are consistent with the standing wave solution, namely

- First: The maximum wave elevation $h = h_{max}$ occurs simultaneously everywhere on the shelf;
  [For example at the coast (x=0) at t=0, $h = h^{(0)}_{max} = a$].
- Second: The velocity and elevation variability are 90^{o} out of phase;
- Third: The horizontal velocity is always zero at x = 0;
- Fourth: The maximum elevation $h = h_{max}$ is non-uniform across the shelf.

The magnitude of **a** is determined by applying the boundary condition at $x = -\ell$, which is that the incident ocean wave, with amplitude $\mathbf{a_o}$, must always to be equal to the shelf wave at the edge of the shelf $x = -\ell$. Thus at t = 0,

$$h(-\ell) = a \cos k(-\ell) = a \cos k(\ell) = a_o.$$

or

$$a = \frac{a_o}{\cos k\ell}$$

so that the shelf standing wave solution becomes

$$h = \left(\frac{a_o}{\cos k\ell}\right) \cos kx \cos wt .$$

Note that in this frictionless ocean, this shelf standing wave becomes infinite for the special geometrical cases where $k\ell = \frac{np}{2}$; or where the shelf width ℓ is related to the wave length L according to

$$\ell = \frac{np}{2k} = \frac{nL}{4} \quad .$$

Thus, for example, when the shelf width is ¼ of the wave length (n = 1; $\ell = L/4$), a shallow water wave with a wavelength $L = T\sqrt{gh}$ and frequency

$$f = \frac{1}{T} = \frac{\sqrt{gh}}{4\ell}$$

is "resonant" with the shelf geometry.

Conversely, if the deep ocean is forcing an approximate twice-daily tidal wave (with a period of $T = 4 \times 10^4$ seconds) on a shelf with depth is h = 10m, then the shelf width that will produce tidal resonance is

$$\ell = \frac{T\sqrt{gh}}{4} = \frac{(4 \times 10^4 \text{ s})(10 \text{ ms}^{-1})}{4} = \underline{100 \text{ km}}$$

Thus this highly *idealized model* tells us that a twice-daily (or semidiurnal) deep oceanic tide of frequency will force an infinite amplitude! standing wave on a continental shelf of width ~100 km. In reality, friction (which this model does not include) plus continuity would not permit an infinite amplitude response to ever occur. However amplified tidal responses do occur in various shelf regions of the world's oceans, including the Gulf of Maine and the Argentina shelf.

Tides

The astronomically-forced surface gravitational tide has long wave lengths compared to the ocean depth and thus is an example of a shallow water wave. Tidal waves are strongly "forced" by the motion of the earth relative to astronomy and in that differ from wind-generated surface gravity waves, which run "freely" after being formed. Also the periods of surface tides are large enough to be influenced by the earth's rotation. (Remember that Airy waves were not influenced by Earth rotation because of their short periods.)

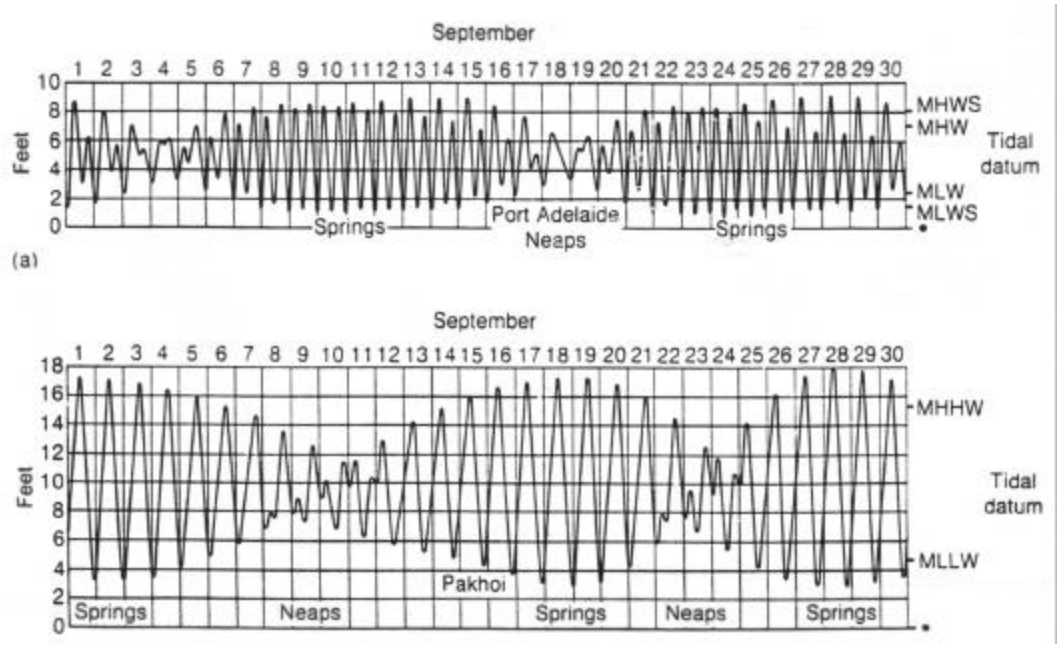

Figure 7.23 Observed tides in Port Adelaide are semidiurnal (twice-a-day) and in Pakhoi diurnal (once-a-day). Tidal ranges in both locations exhibit a spring-neap cycles that are out of phase.

The tidal response of the global oceans is complex because of the combined astronomical *tidal forcing* of the earth, moon and sun. The observed tides differ significantly from location to location because of the shallowness and geographical complexity of the global ocean basins. For example, the tides in Pakhoi, China are primarily once-a-day, while the tides in Port Adelaide, Australia are primarily twice-a-day (Figure 7.23). Although the tides at both locations include both semidiurnal and diurnal tides (note neap tidal variability) respectively but they are too small to detect except when the tidal range is small. Observed tides elsewhere in the world's ocean are composed of differing mixtures of both semidiurnal and diurnal tidal components.

How do we make sense of this complex system? One way is to consider just the semidiurnal tide in the Atlantic ocean and map its lines of constant tidal range (*cotidal lines*) and constant tidal phase (*copahse lines*) on the same picture as shown in Figure 7.24 - a *cotidal chart* for the M_2 semidiurnal tide. This is a classic signature of an *amphidromic system* in the north Atlantic. At its center – the *amphidromic point* - there is no vertical movement of the sea surface.

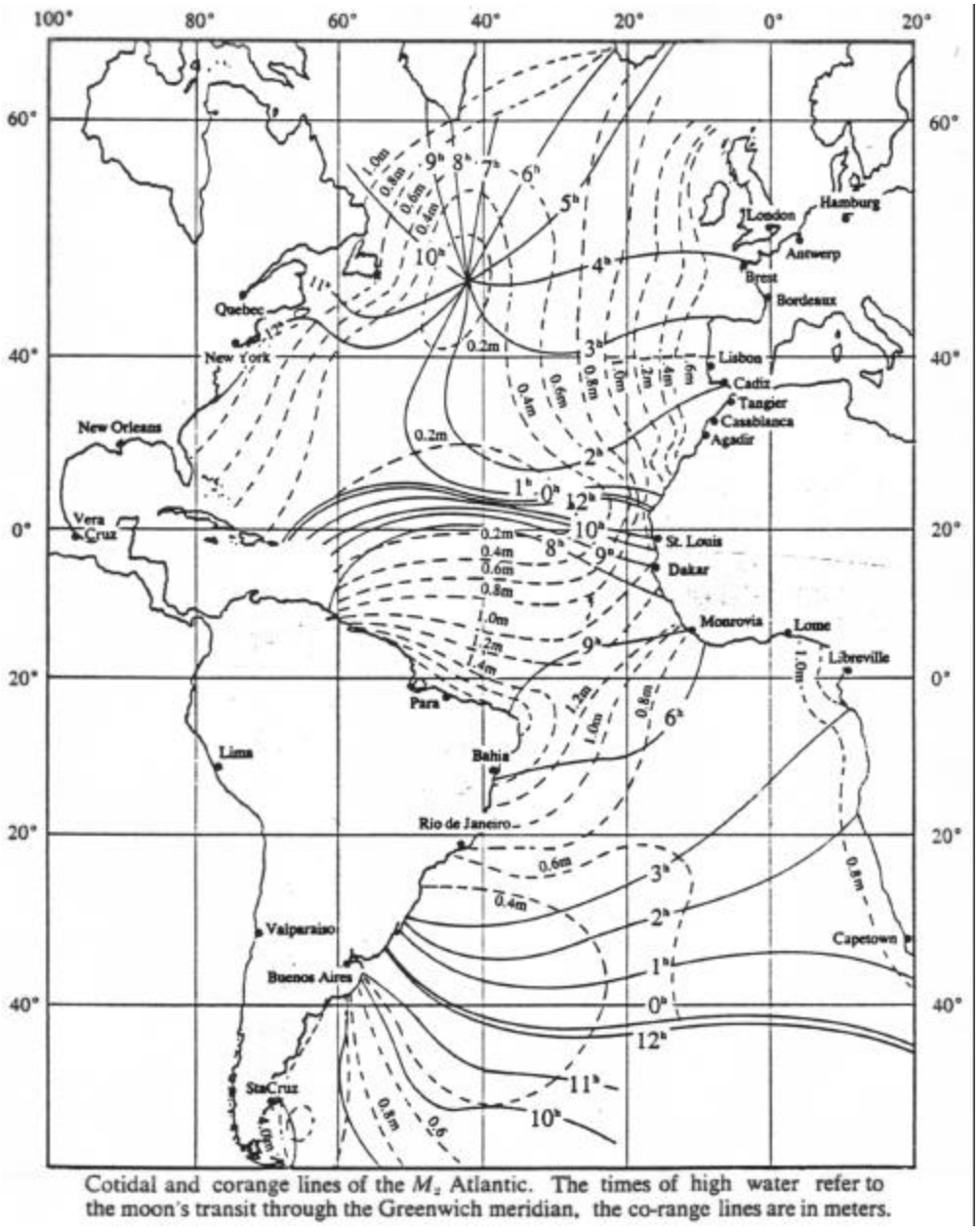

Figure 7.24 A cotidal chart for the M_2 semidiurnal Atlantic Ocean tide. (Thurman, 1975)

The north Atlantic M_2 semidiurnal tidal cotidal chart (Figure 7.24) is a distorted spoke wheel pattern because of the irregular configuration of the continents, variable ocean depths, and friction. The world's ocean tides are just a complicated interaction of several amphidromic systems.

A conceptual model of the north Atlantic amphidromic system is illustrated in Figure 7.25. Moving from A to B to C to D, we see what amounts to a rotary standing wave. This "spoke pattern" of cotidal lines and corange line centering on the hub of the "wheel" is much cleaner in this conceptual model.

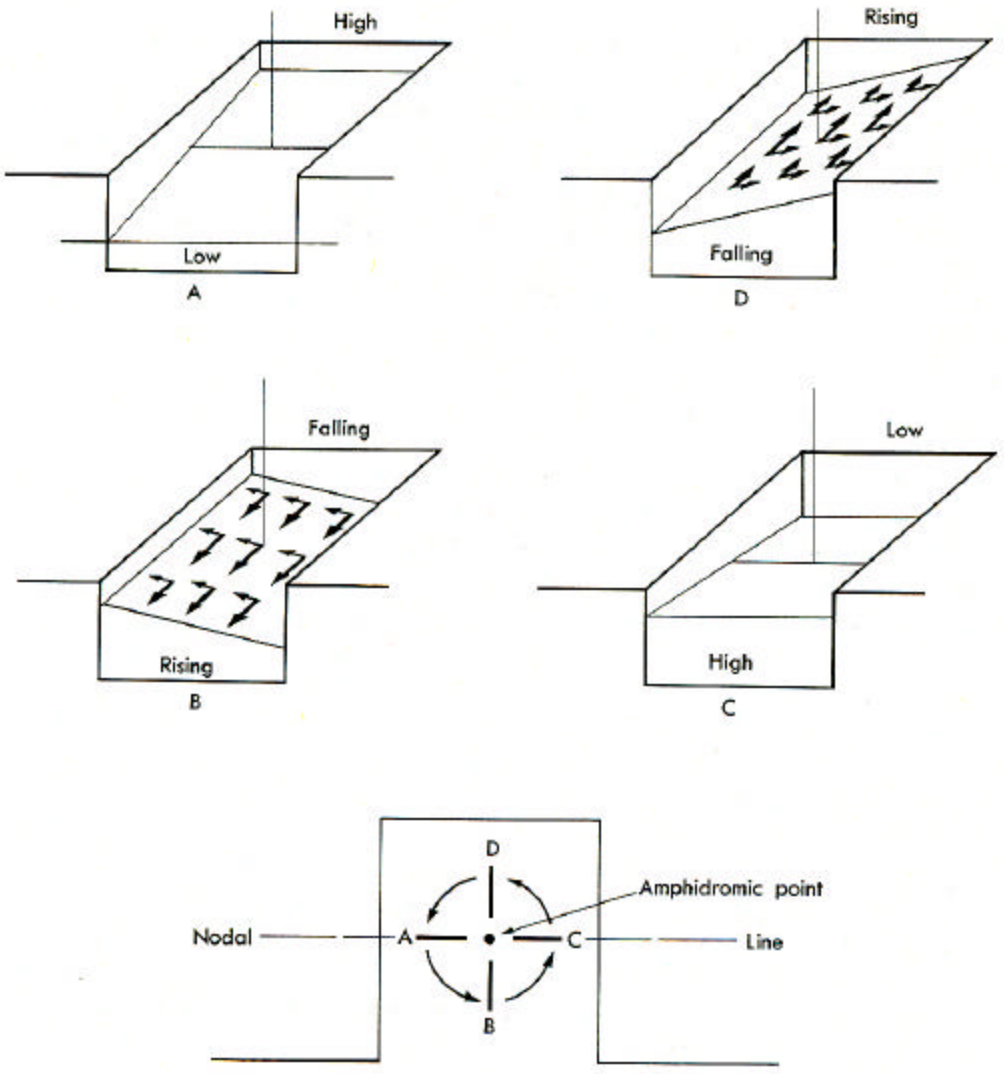

Figure 7.25 Schematic of a rotary tidal amphidromic system. (NOTE D, A, B, and C in the lowest panel should be replaced by A, B, C, D respectively) (von Arx, 1974).

Equilibrium Tides: Rather than trying to deal with the full complexity of real ocean tides, we will investigate the effects of the moon (and sun) on an ocean with a uniform depth that is greater than 25 km and uninterrupted by continents (see Figure 7.26). In contrast to the real ocean, this configuration permits the sea surface distortions produced by the sun-moon gravitational effects to *remain in phase* with the astronomy as the earth rotates below it. This simplified model of ocean tides forms the basis of *equilibrium tidal theory*, which, though unrealistic, helps to explain the origin of the principal frequencies associated with real tides.

The Basic Dynamic System Balance: The moon-Earth (and sun-Earth) gravitationally-forced sea surface distortions vary with latitude and thus can be detected by observers fixed on the rotating Earth. By contrast, the Earth-rotation produced distortions of sea level do not vary with the longitude and thus are not observed. Thus we can assume an irrotational earth-moon system to start the discussion. (The effects of the sun will be incorporated later.)

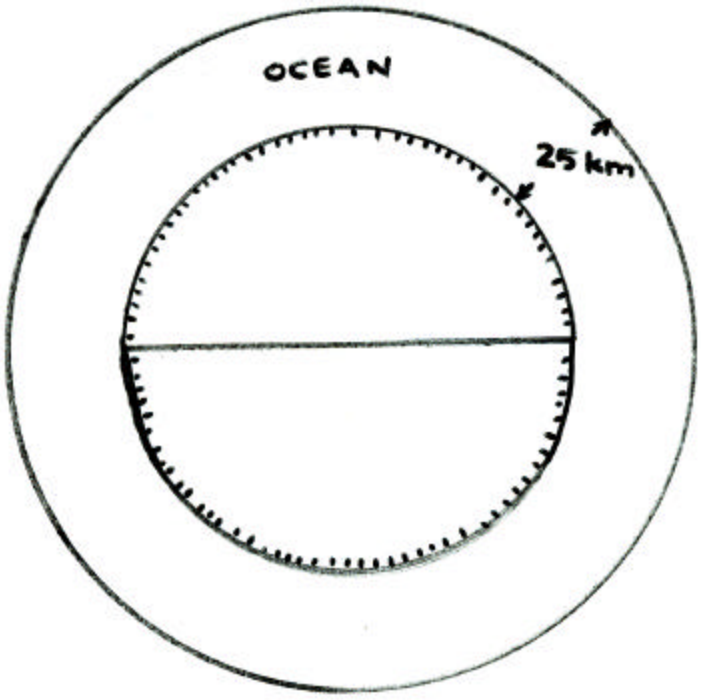

Figure 7.26 Equilibrium tidal ocean with a depth of at least 25 km over the entire Earth.

The earth-moon system rotates at a rate of ω about a point x from the center of the Earth (see Figure 7.27). From a n earth observer's point of view, this basic system dynamic balance is between the gravitational attraction between the moon and earth and the centrifugal "force" associated with the circular motion of the earth's center of mass. This is depicted an alternate way in Figure 7.28.

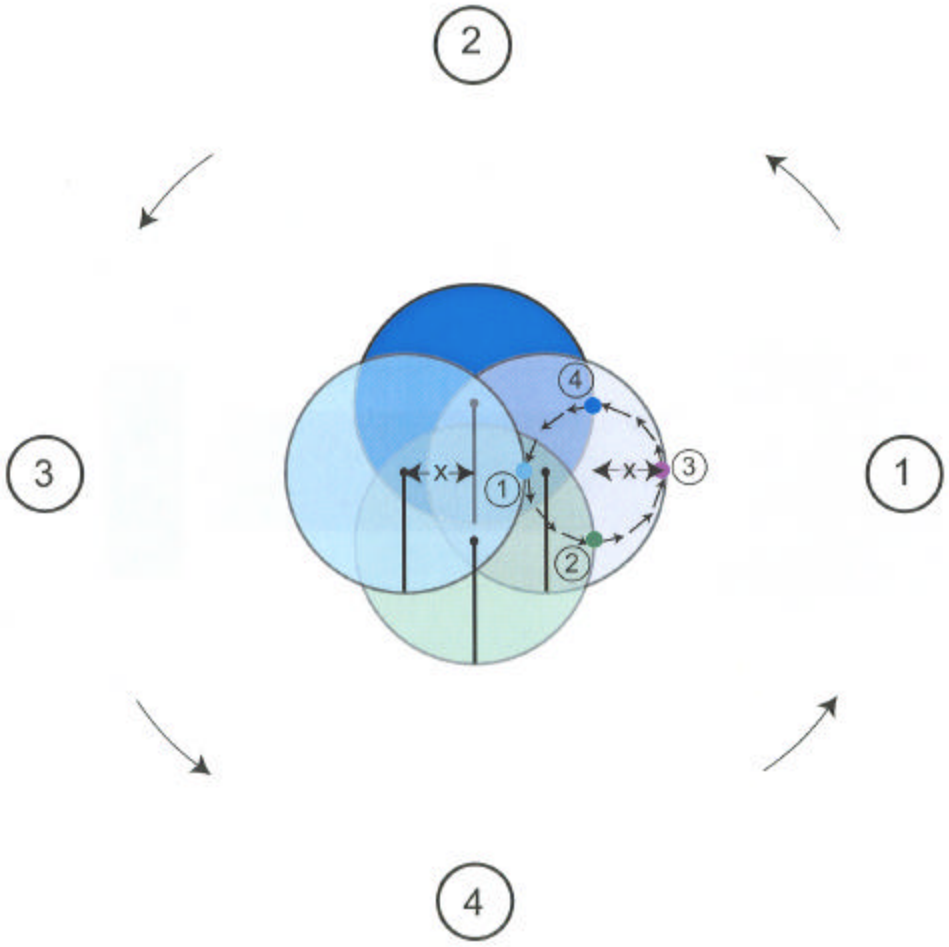

Figure 7.27 To dynamically balance the earth-moon gravitational attraction, both the Earth and the moon rotate around the Earth-moon system center of mass or rotation (SCR - located a distance of x ~ 4600km form the Earth's center). During one monthly counterclockwise (CCW) rotation of system, the SCR traces a circle of radius = x through the irrotational Earth (see main text). Simultaneously the sub-lunar point on the Earth's surface also traces a CCW circle with a radius x; starting at (1- light blue) and progressing through (2 - green), (3 - purple), and (4 – dark blue) and back to (1).

Considering the dynamics of a pair of fluid parcels (each with mass μ) on the surface of an irrotational earth (at **b** and **a** in Figure 7.28). The circular paths of these parcels (as

the earth and moon turn through their monthly cycle) are indicated by the dashed lines in Figure 7.28. This motion occurs because the center of earth-moon system rotation ("spin center" at CG) moves through the irrotational earth.

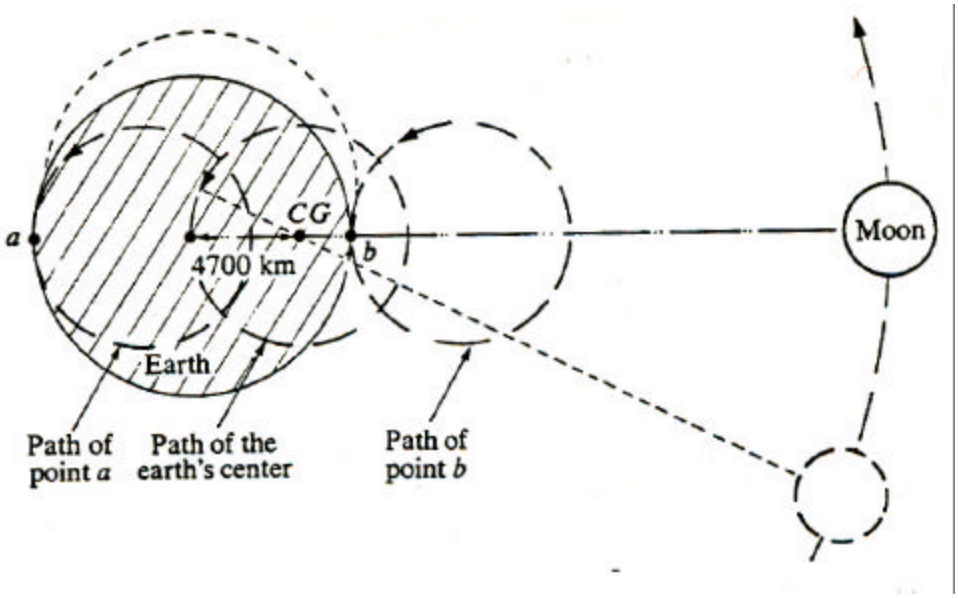

Figure 7.28 The dashed line through the center of the earth is the path of the earth's center as it moves around the common center of gravity (CG) in the earth-moon system. The circular paths followed by points a and b are identical to that followed by the earth's center. (Thurman, 1975)

Mathematically the Earth-moon gravitational force is

$$F_g = G \frac{m_e m_m}{R^2} \quad ,$$

where the gravitational constant is $G = 6.67 \times 10^{-8}$ dyne- cm^2 gm^{-2} ;
Earth mass is $m_e = 5.975 \times 10^{27}$ gm ;
Moon mass is $m_m = 7.343 \times 10^{25}$ gm $= 1/81.56\ m_e$;
Distance between Earth and moon $R = 3.844 \times 10^5$ km ;
Earth radius $r = 6100$ km ;
Distance between Earth & system CM $x = 4700$ km .

The balance between and the Earth-moon gravitational force and the centrifugal force, associated with the system rotation, demands that

$$F_c = m_e w^2 x = G \frac{m_e m_m}{R^2} \quad ,$$

where w is the system rotation rate, which can be determined according to

$$w^2 = \frac{G m_m}{x R^2} = 0.5 \times 10^{-11} \text{ sec}^{-2} \quad ,$$

which corresponds to a system rotation period of T = 27.3 days (sidereal month).

The Tide-producing Force: The *tide-producing force* is the result of imbalances in the basic system dynamic balance discussed above. The distribution of tide producing force over the earth's surface can be determined by considering an array of fluid parcels (with mass = μ) moving in CCW circles (radius x = 4700km) in an inertial frame of reference with centripetal accelerations a_c (see Figure 7.29). As seen by an Earth observer, the total force on each of the fluid parcels is the sum of the gravitational force f_g toward the moon and the centrifugal force $f_c = \mu a_c$ pointing in the opposite direction to a_c and f_g according to

$$f_T = f_g - f_c$$

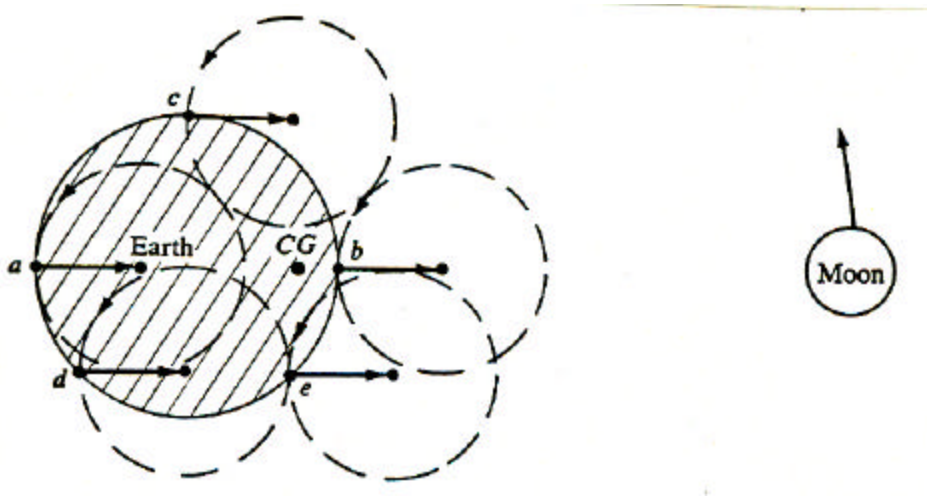

Figure 7.29 The circular orbits of water parcels a, b, c, d, and e maintained by their respective vector *centripetal accelerations*. Note that all of the vectors are *equal!* and thus have equal and opposite *centrifugal force vectors* as viewed by an earth observer. (Thurman, 1975)

The centrifugal force on the parcel, based on the result above, is by definition negative everywhere given by

$$f_c = m\,\omega^2 x = m\,\frac{Gm_m}{R^2}$$

The magnitude of the gravitational force on the parcel varies, depending on whether the parcel is located on the side of the Earth toward the moon and thus R-r distant from the moon; or located on the side of the Earth away from the moon at a distance R+ r according to

$$f_g = \frac{Gm_m\,m}{(R \mp r)^2} \qquad .$$

Thus the total force acting on each parcel is

$$f_T = f_g - f_c = m\,Gm_m\left(\frac{1}{(R \mp r)^2} - \frac{1}{R^2}\right)$$

$$f_T = \frac{m\,Gm_m}{R^2}\left[\frac{R^2 - (R^2 \mp 2rR + r^2)}{(R \mp r)^2}\right]$$

$$f_T = \frac{m\,Gm_m}{R^2}\left[\frac{[\pm 2(r/R) - (r/R)^2]}{[1 \mp (r/R)]^2}\right]$$

Since $r/R \sim 1/60 << 1$, $(r/R)^2$ can be neglected relative to other terms and

$$f_T \sim \pm\, m\,Gm_m\,\frac{2r}{R^3}$$

where (+) indicates that $f_g > f_c$ at the *sub-lunar point* and (-) above indicates that $f_c > f_g$ at the *antipode*.

The basic result here is that the *tide-producing force* (TPF) is <u>proportional to the inverse cube of the earth-moon separation distance</u>. Thus the tide-producing force decreases more rapidly than does the gravitational force itself. As a consequence of this result, the sun's TPF is only 43% of the moon's TPF despite its far greater mass. This is illustrated by the following calculation

$$\frac{f_T^{sun}}{f_T^{moon}} = \frac{m_{sun}}{m_m}\frac{R_{moon}^3}{R_{sun}^3} = 0.43$$

The distribution total TPF at the surface of the Earth (or our equilibrium tidal ocean) is illustrated for a general Earth-moon orientation at some arbitrary angle relative to the Earth's equator in Figure 7.30a. Note that on the side of the Earth facing the moon that $f_g > f_c$ and away from the moon $f_c > f_g$.

The TPF can be resolved into its local vertical (z) and tangential components. The magnitude of the vertical component of the TPF is very small compared to gravity (the order of 10^{-7} g) and thus has a negligible effect in producing tides. However, distributions of the tangential component of the TPF - called the *tractive force* - acts effectively on the mobile water to produce the double bulge in ocean sea level seen in Figure 7.30b. (On tidal time scales the earth can respond elastically and thus the TPF tractive forces also produce solid "earth tides").

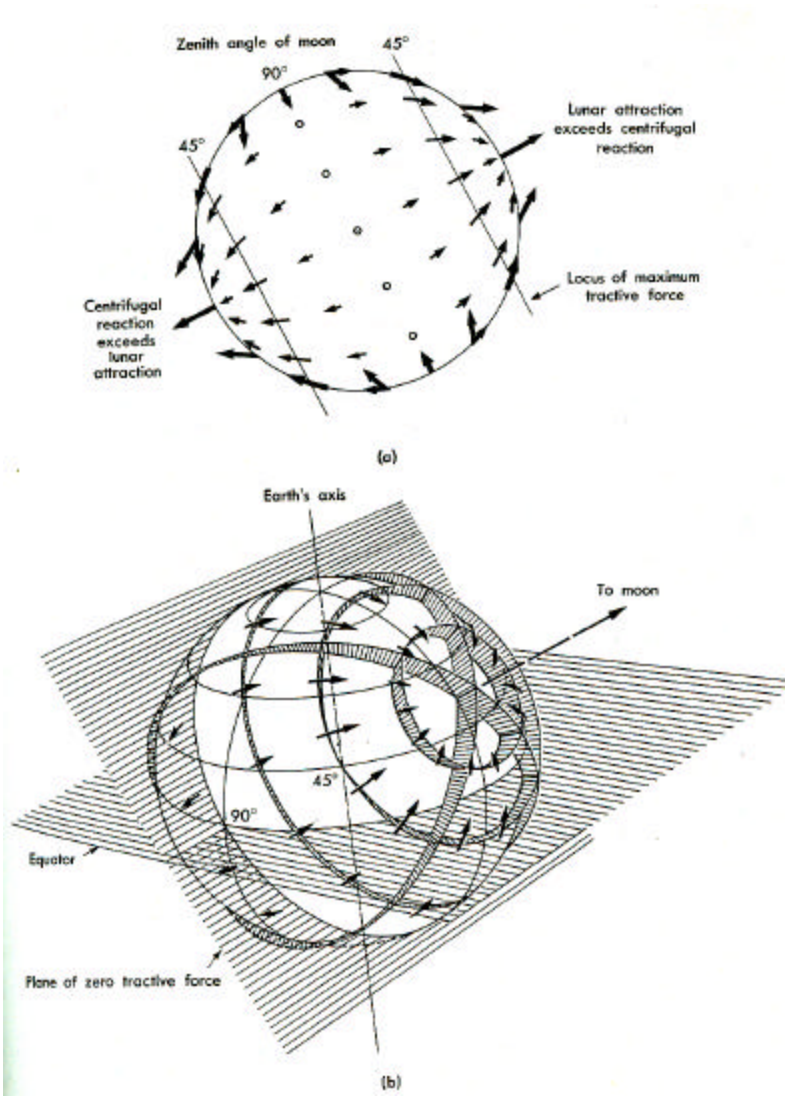

Figure 7.30 (a) The distribution of the tide-producing force TPF; it is dominated by f_c on the side of the Earth facing away from the moon and by f_g on the side facing the moon. **(b)** The distribution of the tangential component of the relatively small TPF - the tractive force – varies over the Earth's surface, reaching its maximum value along two circles which lie at 45 ^{o} relative to the plane of the earth-moon (or sun system). The tractive force is unopposed and causes the two equal sea surface "bulges" on either side of the Earth (hatched). (Neshyba, 1987)

This distribution produces a *double tidal bulge* (as indicated above) which remains stationary relative to the earth which rotates beneath. There are a number of interesting consequences of this set of circumstances, namely

1) *Two high tides* are observed each *a lunar day*, which is $24^{h}\ 50^{m}$. The extra 50^{m} is the time of the extra earth rotation that is needed to "catch up" to the moon. The moon moves 12.2 ^{o} (= $360°/29.53^{d}$) every solar day as it

"revolves" about the earth in a 29.53^{d} *synodic* or *lunar month (*defined as the time from new moon to new moon). Figure 7.31 shows the difference between a sidereal and lunar month.

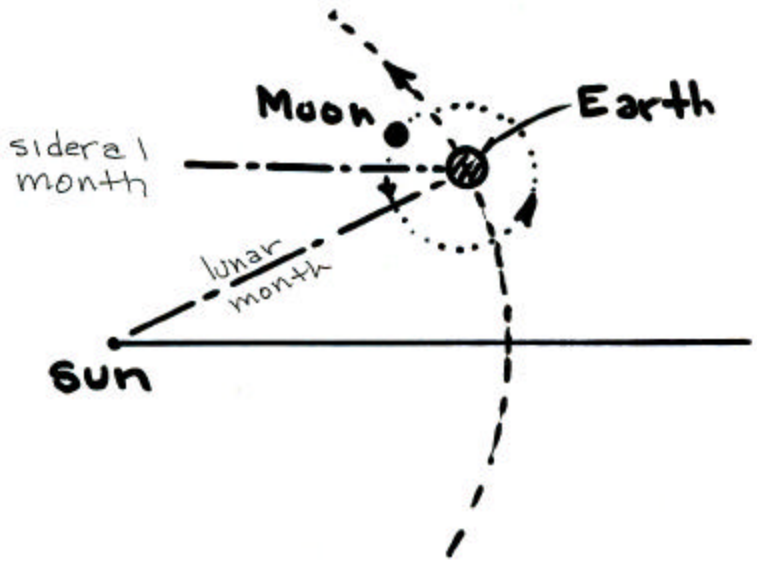

Figure 7.31 The sidereal and lunar month differ by the time it takes for the moon to move so that it is overhead at "solar noon".

2) *Equatorial tides* occur two times during the month when the moon passes through the plane of the earth's equator (i.e. the sub-lunar point is located at the earth's equator – see Figure 7.32). At these times, the *twice-a-day* or *semidiurnal tides* have equal amplitudes.

3) Normally the double tidal bulge is oriented at angles to the earth's equator and the semidiurnal tide has different amplitudes during a lunar day (see Figure 7.32). The amplitude difference between the semidiurnal tides is known as the

once-a-day or *diurnal inequality.*

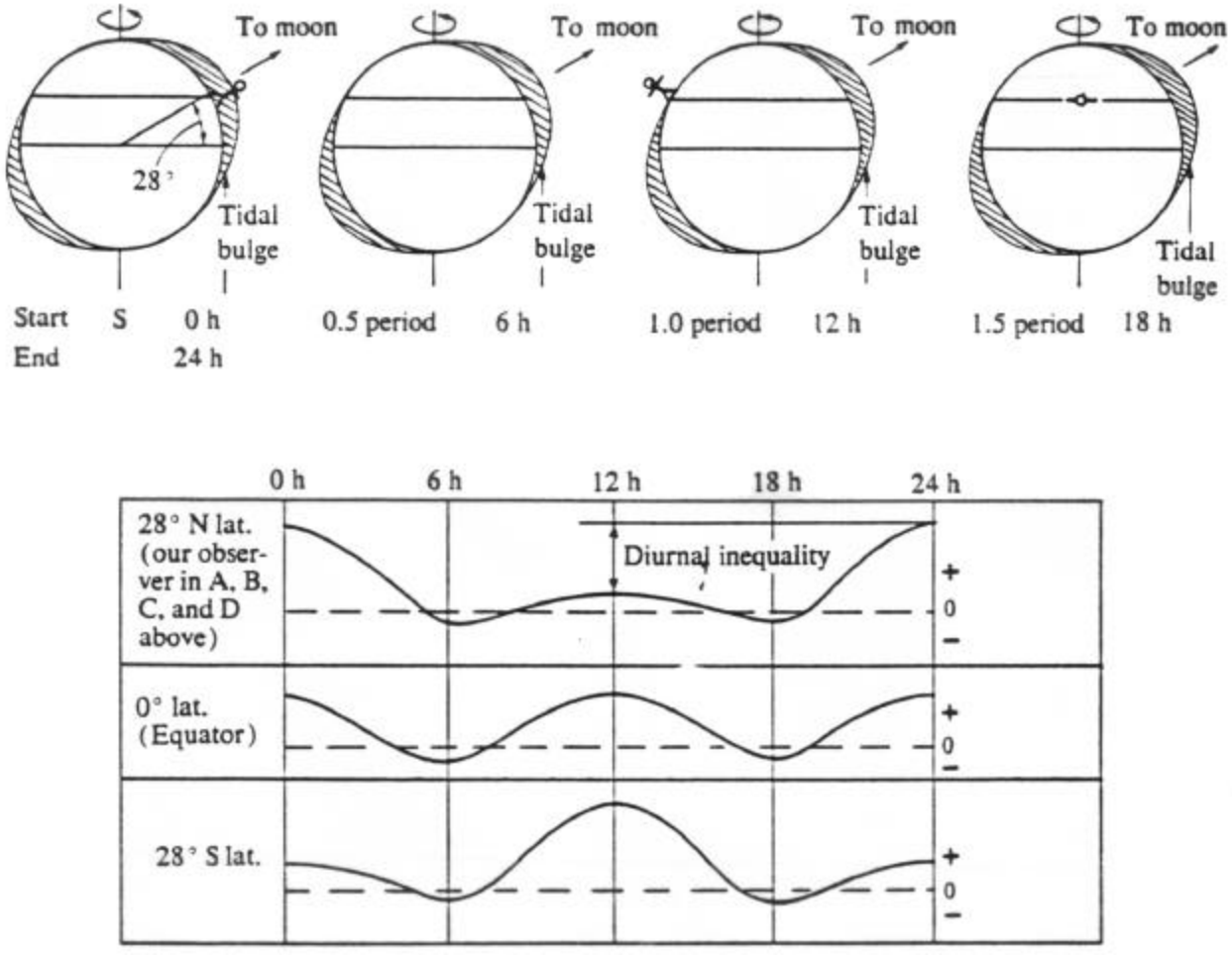

Figure 7.32 An observer on a rotating earth sees two high-water marks during one rotation. In the special cases two times a month, when the moon is in the equatorial plane, all earth observers will see two equal amplitude high tides -called equatorial tides - each lunar day. Generally, however, the two high tides are of unequal heights –hence a diurnal inequality. These cases are illustrated in the lower panel with typical sea level records during one rotation of the earth. Note that the equator, the two high tides are always of equal amplitude. (Thurman, 1975).

4) When the sun and the moon are in *conjunction* or *opposition* (Figure 7.33) their tide-producing effects reinforce to produce *spring tides* of maximum tidal range twice each month. When the moon and the sun are in *quadrature* their tide-producing effects compete to produce *neap tides* of minimum tidal range *twice each lunar month.*

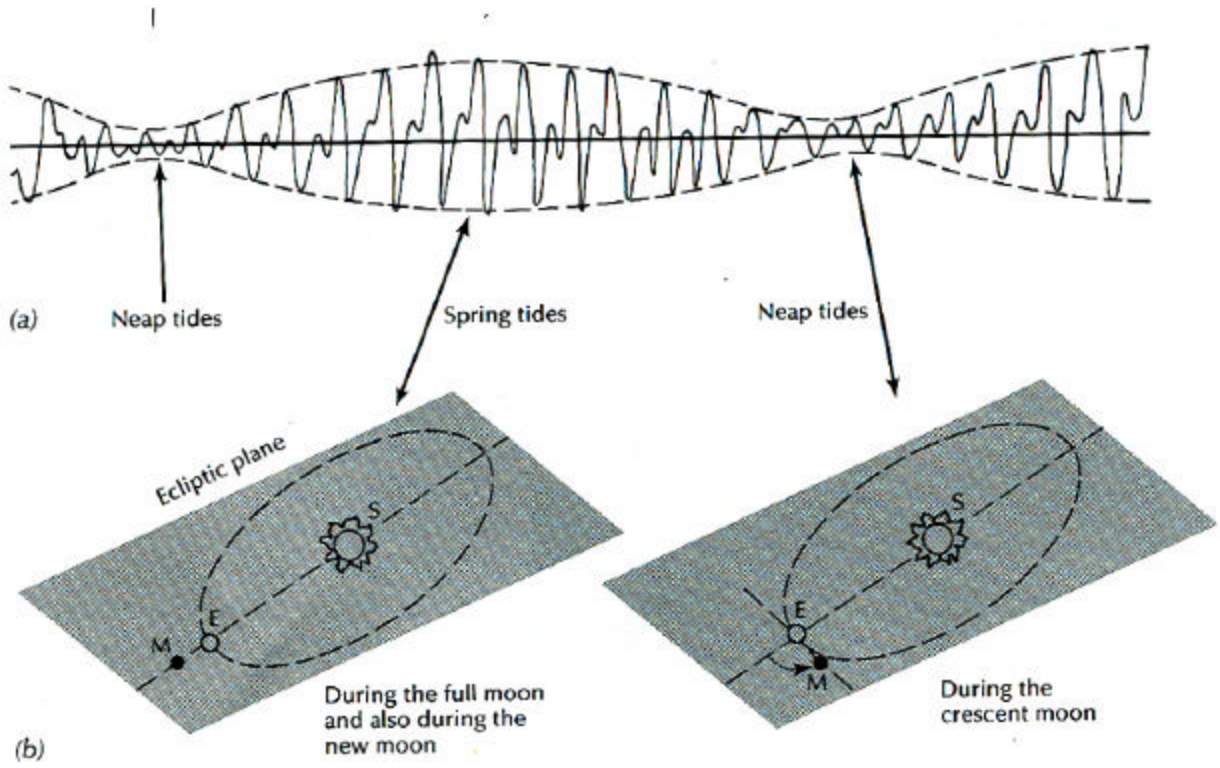

Figure 7.33 (a) A monthly tidal record highlighting the spring-neap tidal amplitude envelope, which results from **(b)** the monthly astronomical interactions of the lunar and solar tidal forcing or the "beating" of the lunar and solar tidal forcing cycles.

5) Changes in the *declination* of the orbits of the earth ("around the sun") and moon ("around the earth") produce subtler changes in the tide-producing forces. For example,

(a) An *annual cycle* in the tides occurs because the earth rotation axis is tilted 23.5^{o} relative to the plane of the ecliptic (i.e. the plane of the sun-earth system). Thus, as the earth "orbits" the sun (see Figure 7.34), the declination of the sun relative to the earth's equator changes from latitude 23.5^{o} N at the summer solstice to 23.5 ^{o} S at the winter solstice.

(b) An *18.6 year cycle* occurs because the plane of the earth-moon rotation system precesses relative to the ecliptic plane. Thus the declination of the moon relative to the earth's equator changes from

18.5 ^{o} to 28.5 ^{o} during this period.

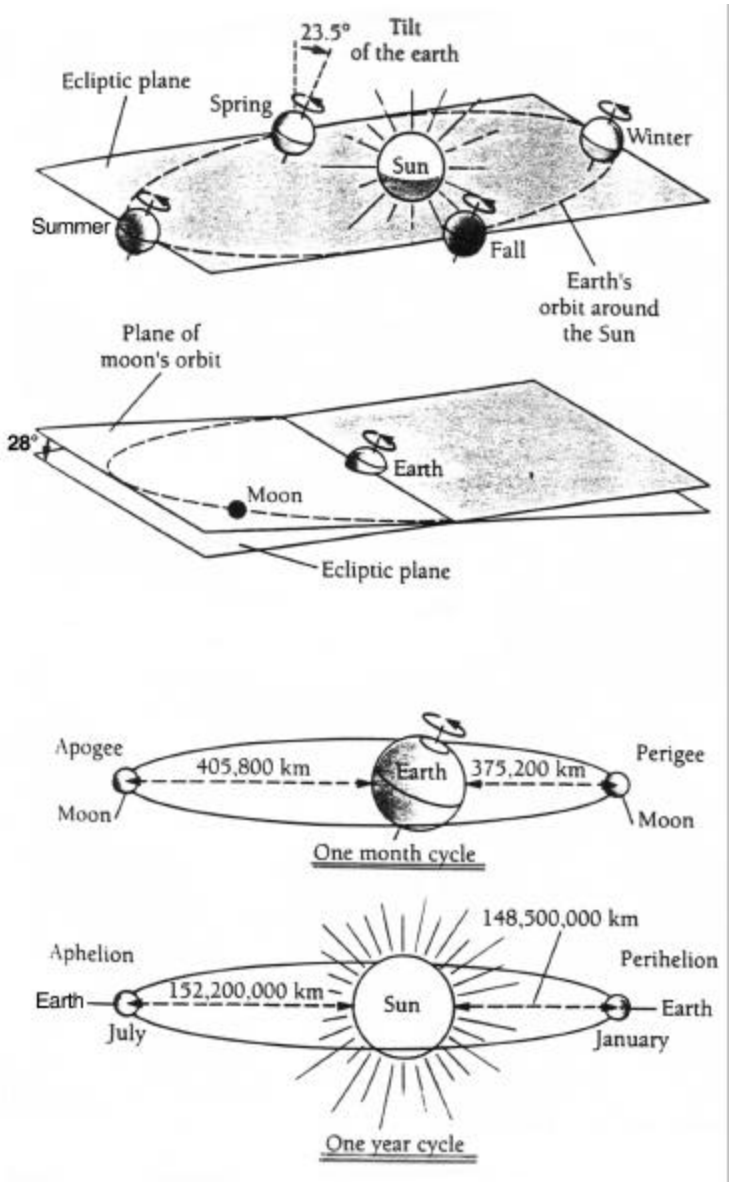

Figure 7.34 (upper panel) An *annual tidal cycle* arises because of the 23.5 ^{o} inclination of the earth's axis relative to the plane of the earth-sun (plane of the ecliptic). **(upper middle panel)** An *18.6 year tidal cycle* arises because the plane of the earth-moon rotation precesses. **(lower middle panel)** A *monthly tidal cycle* arises because of earth-moon separation changes. **(lower panel)** Another *annual tidal cycle* arises because of earth-sun separation changes.

6) Changes in the *distance* between the earth and moon and earth and sun produce changes in the tide producing force (proportional to $1/R^3$). Thus there are observable changes in the tides due to the ellipticity of the moon's orbit around the earth and the earth's orbit around the sun (see Figure 7.34). For

example,

(a) An *anomalistic month*ly cycle (27.5 solar days) the moon moves from *perigee* (at 375,200 km from the earth) to *apogee* (at 405,800 km) and back again.

(b) A *yearly cycle* as the earth moves from *perigee* relative to the sun to *apogee* and back again.

7) There are even longer period tides, which result from other astronomical variations including the 100,000 year cycle in the eccentricity in orbit of the earth "around the sun".

Thus the earth's oceanic tidal variability reflects by the different tones (i.e. frequencies) of the earth-moon-sun gravitational interactions. It turns out that all important *tidal frequencies*, can be defined in terms of the six *principal frequencies* defined in the Table 7.1.

Table 7.1 The six principal frequencies of ocean tides.

Source	**Angular Frequency**
earth rotation	$w_t = \frac{2p}{\text{lunar day}} = 360^o - 12.2^o/\text{d}$
lunar revolution	$w_s = \frac{2p}{\text{sidereal month}} = 13.176^o/\text{d}$
solar declination	$w_h = \frac{2p}{\text{solar year}} = 0.985^o/\text{d}$
revolution of lunar perigee	$w_p = \frac{2p}{8.87 \text{ years}} = 0.111^o/\text{d}$
precession of lunar node	$w_N = \frac{2p}{18.6 \text{ years}} = 0.0529^o/\text{d}$
revolution of solar perigee	$w_{p1} = \frac{2p}{20{,}000 \text{ years}} = 0.00005^o/\text{d}$

The ocean tide anywhere on the earth can be decomposed into 400 *partial tides* (or *tidal species*) each with a unique frequency w_i that can be expressed in terms of these principal frequencies such that

$$w_i = a_1 w_t + a_2 w_s + a_3 w_h + a_4 w_p + a_5 w_N + a_6 w_{pl}$$

where a_i are a set of six *integer coefficients* (where i = 1,2,3,4,5, & 6). Doodson developed a shorthand notation for the different tidal species called the Doodson number. For example, the interaction of lunar declination changes and the earth's rotation lead to the pair of frequencies $w_t + 4w_s$ and $w_t - 4w_s$ (as explained below); with Doodson number specifications (1 4 0 0 0 0) and (1 - 4 0 0 0 0) respectively.

Physically these many different partial tides and their frequencies arise out of the nonlinear interactions of the different astronomical forcings and the rotating earth.

In Figure 7.35 the moon is declined relative to the earth's equator - with colatitude Δ. We seek to compute the tide-producing force at a general point **p** with a colatitude q. The longitude difference between the sub-lunar point and point **p** is angle a; which changes with time at a rate w_t according to

$$a = w_t\, t = 2p\, \frac{(t - t_o)}{T_L},$$

where T_L is the lunar day period = $24^h\ 50^m$ (and $\underline{I = \tau}$). Colatitude angle ? also changes with time, but at the slower rate w_s.

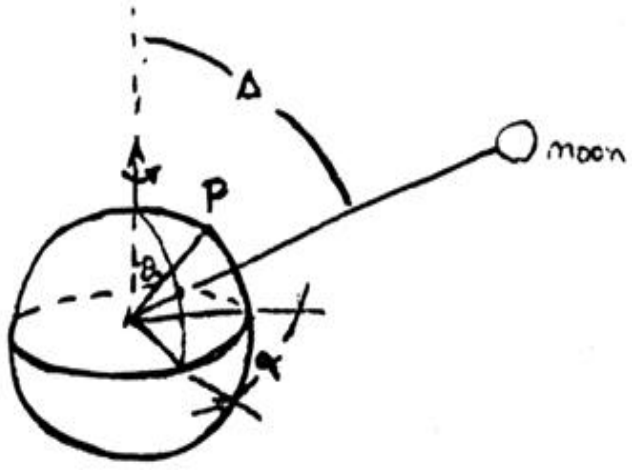

Figure 7.35. The general geometrical configuration of the moon-earth tide-producing force case.

It can be shown that the tide-producing force F_T at an arbitrary point **p** is

$$F_T \; a \; \frac{m_m}{R^3}\{\frac{3}{2}(\cos^2\Delta - \frac{1}{3}) \qquad \text{(long period)}$$

$$+\frac{1}{2}\sin\ 2\Delta\cos w_t\, t \qquad \text{(diurnal)}$$

$$+\frac{1}{2}\sin^2\Delta\cos 2w_t\, t\} \qquad \text{(semidiurn al)}$$

where again $\underline{I = \tau}$.

Expanding the $\sin\ 2\Delta$ term in the diurnal component of F_T yields

$$F_T^D \; a \; \frac{1}{2}\ \sin\ 2\Delta\cos w_t\, t$$

$$a\ \frac{1}{2}\cos(4w_s t)\cos(w_t t)$$

$$a\ \cos(w_t + 4w_s)t + \cos(w_t - 4w_s t)\,.$$

where $I = \tau$.

Thus a spectrum of the tide producing force does <u>not</u> one peak at w_t , but rather a double peak at $w_t \pm 4w_s$ respectively.

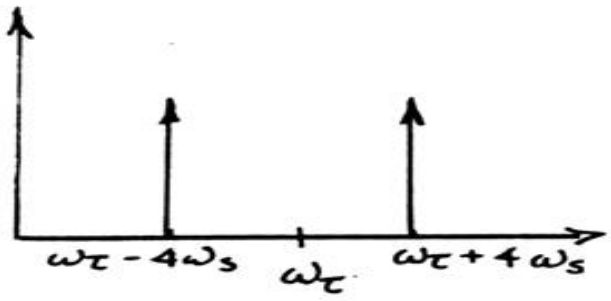

Figure 7.36 Line spectrum of two tidal constituents.

Likewise the *nonlinear interactions* among other periodic tide-producing components leads to additional characteristic frequencies.

Thus the total tide-producing force can be conceptually modeled as the combined contributions of a suite of separate astronomical bodies orbiting a non-rotating earth, each with its own characteristic frequency, w_i. Each astronomical body produces a *partial tide* T_i according to

$$T_i = A_i \cos(w_i t + e_i) \quad ,$$

where the subscript i is the body ID, A_i is the partial tidal amplitude and e_i is the reference phase. We will use this model to describe the real ocean tides.

While the equilibrium tidal theory is useful in describing the ocean tidal forcing, it does not explain the actual ocean tides as they are observed on the earth. (It actually explains earth tides better). As discussed above, restricted depths, friction and continental blockage produce a deep ocean response to the astronomical tidal forcing that is a complicated set of interacting amphidromic systems (e.g. Figure 7.24). The tides on the continent shelves, in coastal regions and in estuaries usually are forced by the deep ocean tide and are modified even further by geometrical, non-linear fluid and frictional effects.

Nevertheless the characteristic frequencies in the equilibrium tide are present in the observed tides nearly everywhere. Because of this fact, people were able to develop predictive schemes for tides about 200 years ago... long before we understood their

dynamics. The empirical means used to make these tide predictions is the next subject to be discussed.

Harmonic Analysis of Tides

Because the astronomical forcing of tides is essentially constant, it is possible to decompose a long record of sea level observations at a particular location into a unique set of partial tidal components or *tidal constituents* defined according to

$$h_i = H_i \cos(w_i t + k_i);$$

where the pair of harmonic constants H_i (amplitude) and k_i (phase) at *each* w_i are determined using the observations and least squares fitting techniques. The i pairs of harmonic constants (H_i, k_i) are used to produce a prediction of tidal sea level change at *that* station according to

$$h(t) = \sum_i h_i = \sum_i H_i \cos(w_i t + k_i).$$

For most purposes, less than 10 constituents are required to describe the tide adequately at a particular station. An example of a harmonic analysis of tides is presented in Figure 7.37 and Table 7.2. Note that this method is useful in predicting only that part of the sea level fluctuation which (1) occurs at astronomical frequencies and (2) is phase-locked to the astronomical forcing. The non-tidal residual signal is due to other oceanic processes including weather forced phenomena, hydrodynamic non-linearities, ($(\vec{V} \bullet \nabla)\vec{V}$ terms) and wave phenomena at non-tidal frequencies. Fortunately the principal contribution to sea level change is usually the tides so that harmonic analysis is widely useful. The harmonic analysis of ocean currents is more difficult because these are significant ocean currents at tidal frequencies which are not phase-locked to astronomical forcing. Thus currents are more "noisy" when it comes to extracting the astronomical tide using harmonic analysis. Internal gravity waves, which we discuss briefly next, represent one of the principal "contaminants" of the tidal currents.

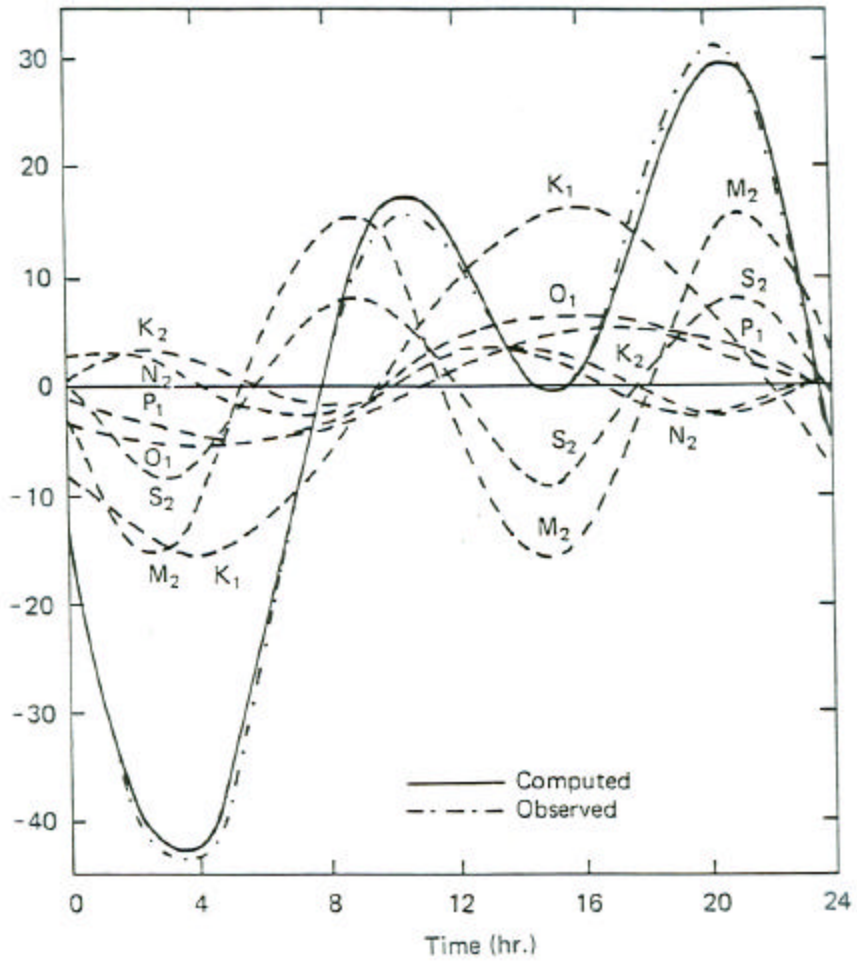

Figure 7.37 Harmonic decomposition of an observed sea level record (dash-dot) into several constituents, which when added yield the computed (solid) predicted tide.

Table 7.2 Partial harmonic components of the composite tide

Name of Partial Tides	**Symbol**	**Speed** (degrees per mean solar hour)	**Period** (solar hours)	**Coefficient Ratio** $M_2 = 100$
Semi diurnal Components				
Principal lunar	M_2	28.98410	12.42	100.0
Principal solar	S_2	30.00000	12.00	46.6
Larger lunar elliptic	N_2	28.43973	12.66	19.2
Luni-solar semidiurnal	K_2	30.08214	11.97	12.7
Larger solar elliptic	T_2	29.95893	12.01	2.7
Smaller lunar elliptic	L_2	29.52848	12.19	2.8
Lunar elliptic second order	$2N_2$	27.89535	12.91	2.5
Larger lunar evectional	$?_2$	28.51258	12.63	3.6
Smaller lunar evectional	$?_2$	29.45563	12.22	0.7
Variational	μ_2	27.96821	12.87	3.1
Diurnal Components				
Luni-solar diurnal	K_1	15.04107	23.93	58.4
Principal lunar diurnal	O_1	13.94304	25.82	41.5
Principal solar diurnal	P_1	14.95893	24.07	19.4
Larger lunar elliptic	Q_1	13.39866	26.87	7.9
Smaller lunar elliptic	M_1	14.49205	24.86	3.3
Small lunar elliptic	J_1	15.58544	23.10	3.3
Long-Period Components				
Lunar fortnightly	M_1	1.09803	327.86	17.2
Lunar monthly	M_m	0.54437	661.30	9.1
Solar semiannual	S_{sa}	0.08214	2191.43	8.0

Other Ocean Waves

Internal Waves

Thus far we have considered surface gravity waves, which have a significant expression at the air-sea interface. The density difference between air and water (in a ratio of about 1/800) leads to a gravitational restoring force for fluid which is displaced vertically. Though density differences are much less at depth, a similar restoring force is present and *internal gravity waves* are possible. The surface expression of internal waves is very small, hence the name.

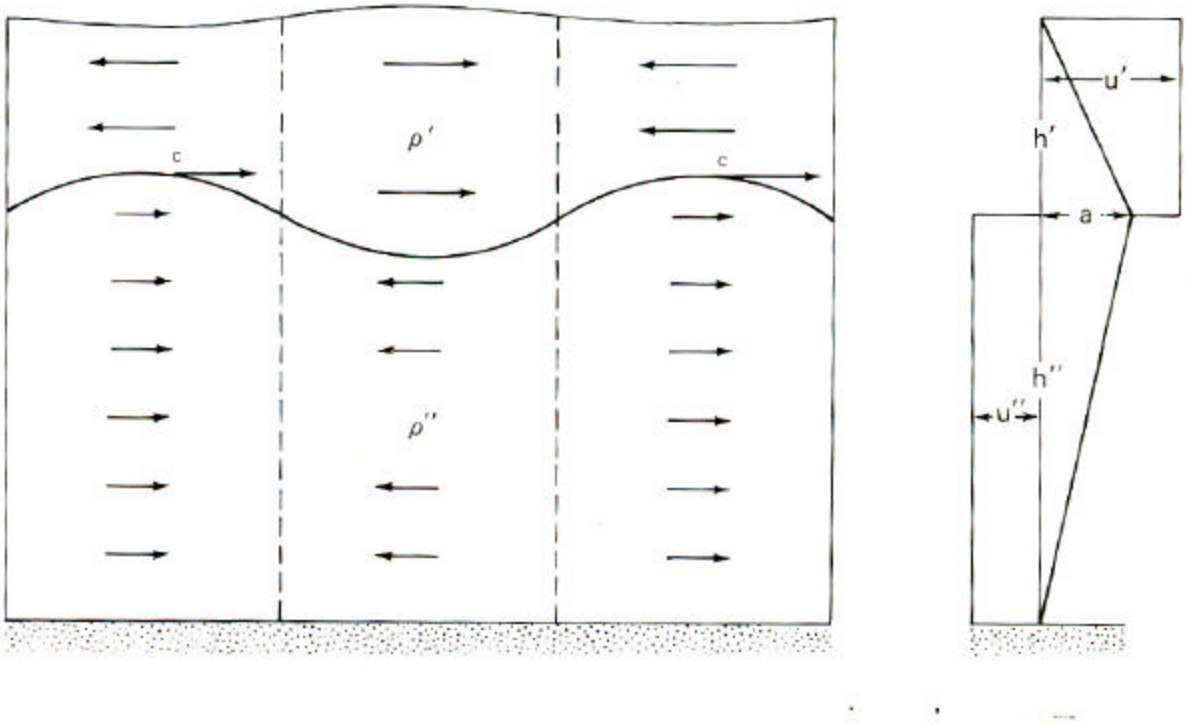

Figure 7.38 Configuration of an interfacial internal waves.

Consider the case in Figure 7.38, where a less dense (ρ') thin layer (h') overlies a deeper layer (h'') of slightly more dense water (ρ'') (Figure 7.37). Theory indicates that the internal wave of wave length L has a phase speed of

$$c = \{gh' \left(\frac{r'' - r'}{r''}\right)\}^{1/2}$$

where $L/20 > h'$ and $L/2 < h''$. Thus the "shallow water" internal wave speed is considerably less than its surface water counterpart because the reduced density differences decrease the effect of gravity as indicated.

In most of the ocean, the density varies more smoothly with depth and the more complicated corresponding theoretical analysis indicates that internal waves can occur at all depths, where there is stable vertical density profile. Frequencies of these internal waves can vary between an upper limit of the local buoyancy (or Brunt-Viäsäla) frequency, N(z) and a lower limit of the local Coriolis parameter $f(f) = 2\Omega \sin(f)$. The distribution of internal wave energy is determined by the differing forcing mechanisms that are relevant.

An important example is the role of *barotropic tidal currents* – associated with the surface tide- impinging on the bathymetric slopes such as Stellwagen bank in Massachusetts Bay. A set of temperature measurements that we made in the deep ocean off Southern California showed a concentration of energy at semidiurnal frequencies. The principal *temperature fluctuations* were due to internal waves of tidal frequency, with *amplitudes* of nearly 100 m and *wavelengths* of about 100 km.

Although this set of observations revealed particularly large internal tides (because it is generated nearby), it has been shown that internal tides represent an important component in the internal wave field everywhere in the world's oceans.

Satellite observations of the sea surface indicate that coastal ocean has important areas of internal tide generation and propagation. This mechanism for internal tidal generation also is found locally in Massachusetts Bay. An array of moored temperature and conductivity measurements near Stellwagen Bank have been used to compute density time series at 6 levels. Using linear interpolation techniques, we produced the suite of isopycnal displacement time series shown in Figure 7.39.

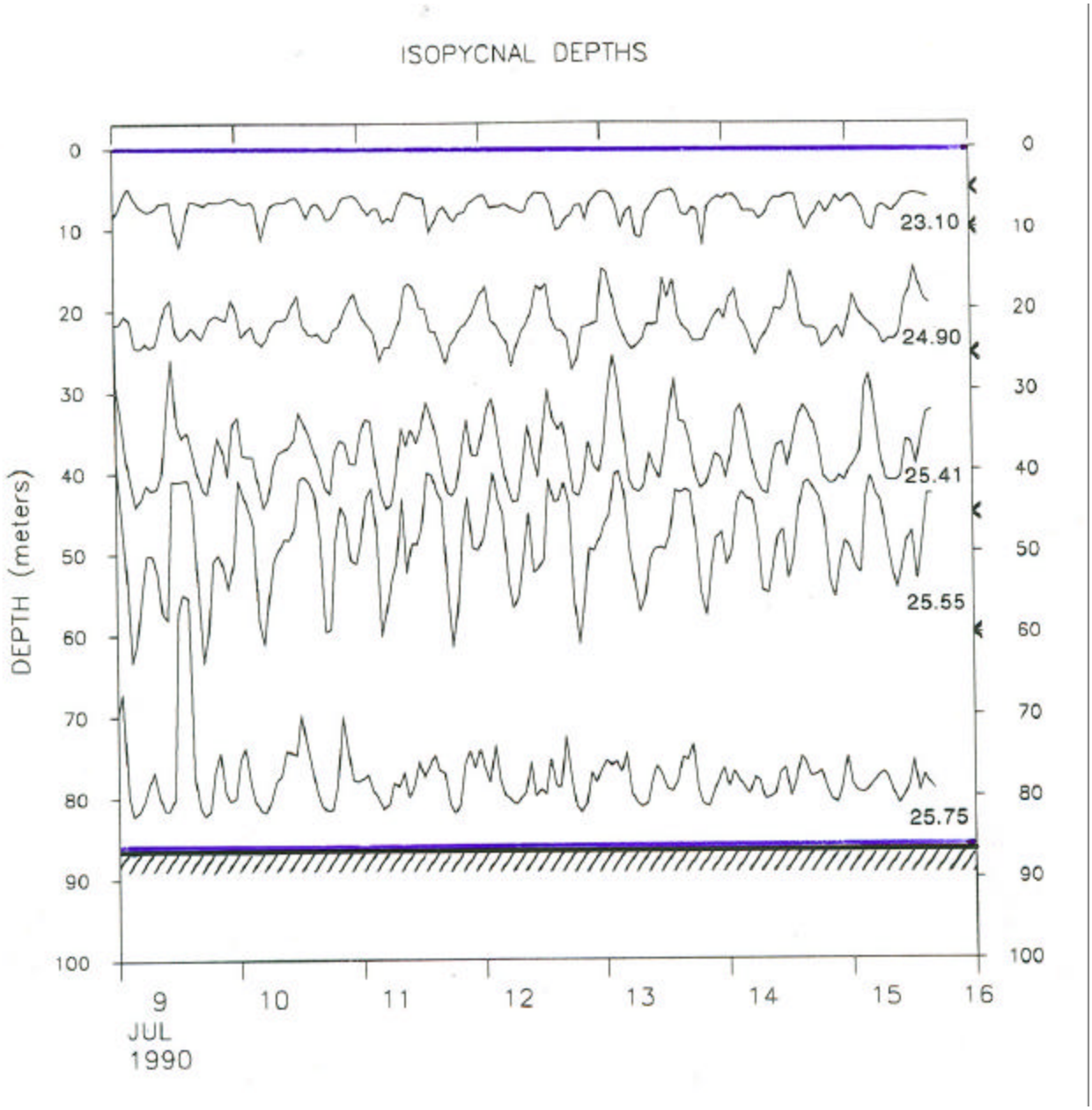

Figure 7.39 Isopycnal depth time series – inferred from density measurements - indicate strong internal tidal signatures throughout the water column

The energy spectra of these time series in Figure 7.40 clearly indicate the importance of the internal tide in the region.

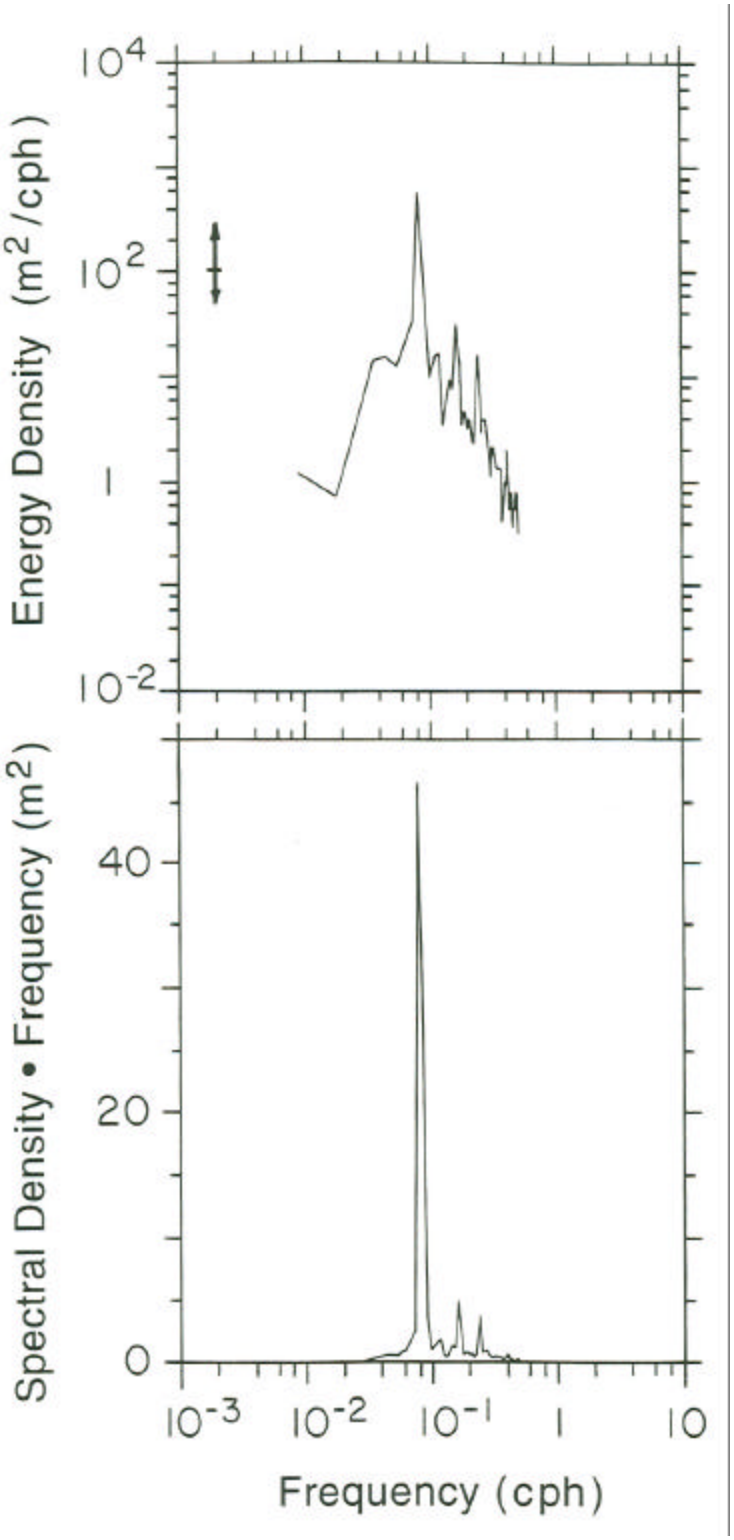

Figure 7.40 (above) Isopycnal displacement energy density spectrum. The prominent peak in the semidiurnal (~12hr) frequency band is consistent with the proximity of the measurements to the internal tidal generation zone on Stellwagen Bank. (b) Variance-preserving spectrum of the isopycnal displacement energy indicates the dominance of the semidiurnal internal tidal energy in the 12 hour frequency band.

An analysis of these data has enabled us to construct the kinematical picture of the isopycnal displacement and current structure in Figure 7.41. Note the zones of horizontal current convergence in the upper water column (strongest at the surface) and divergence at depth leading the isopycnal wave crest as it propagates from right to left. The current shear associated with such wave motion can become unstable leading to internal wave breaking and mixing. Studies indicate that *breaking internal waves* in bathymetric slope regions may be important mechanisms for resuspending the sediments that form the sea floor in these regions.

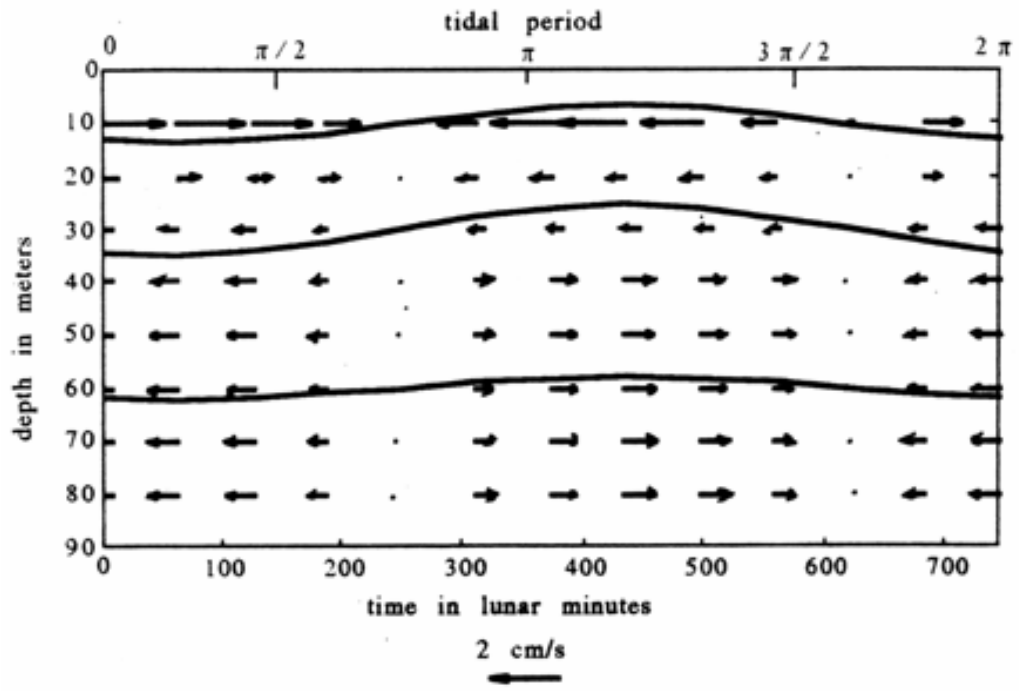

Figure 7.41 Internal Wave Kinematics: The spatial distribution of isopycnal displacement (-) and horizontal velocities associated with one cycle of am M_2 internal tidal wave in an ocean with exponentially decreasing $N^2(z)$.

Planetary Waves

This class of waves are generally found at periods greater than a day and are due to the effects of a Coriolis parameter, $f = 2w \sin f$, which varies with latitude. Its dynamics can be illustrated by considering the movement of a column of water northward in a frictionless, constant depth ocean. As f increases the water column will exhibit

increased negative relative vorticity and will circulate clockwise.

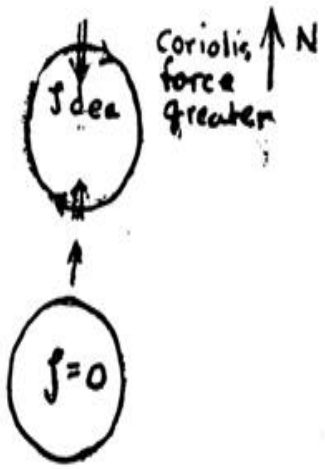

Figure 7. 42. Vorticity change associated with a northward displacement of a large ocean parcel. Note that the flow is quasigeostrophic.

The Coriolis force at the northern extremes of our column will be greater than that at the southern extreme. Thus there will be a southward restoring tendency. If the column is pushed southward through the latitude of zero relative vorticity then V will increase producing anti-clockwise motion and a corresponding northward restoring tendency. Thus the variation of f provides the *horizontal restoring force* for waves whose phase propagates in the west direction according to

$$c_p = \frac{-\left(\frac{\partial f}{\partial y}\right)_o}{k^2} = -\frac{b}{k^2}$$

where k is the wave number.

The group velocity of these dispersive waves can be either east or west. Note that in contrast to surface waves the shorter period waves are the longer wavelength waves and conversely.

Although the dynamics of oceanic planetary waves is similar to those of atmospheric planetary waves their observed wavelengths and frequency range is different. Thus in contrast to the atmosphere where planetary waves play a key role in the dynamics of weather, it is not clear what the role of oceanic planetary waves is. Massive theoretical and experimental efforts begun during the 70's are beginning to reveal the importance of

these motions to energy transfer in the ocean.

We are now at the stage where it is useful to look at the energy density spectrum of oceanic processes. The frequency (actually period) spectrum (Figure 7.43) shows the relationship of the important oceanic processes we have discussed. This type of presentation is useful for illustrating the full dynamic range (in terms of energy and frequency) of these processes.

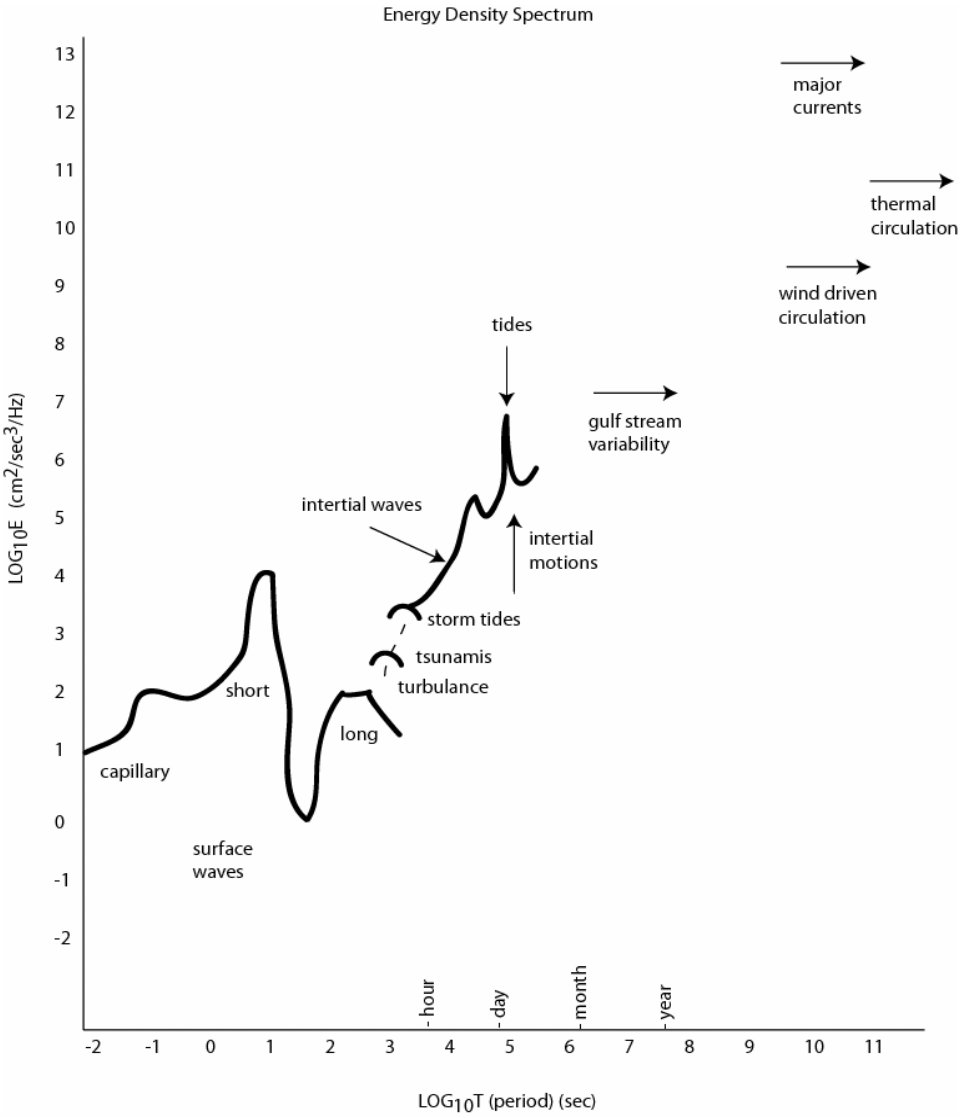

Figure 7.43 Spectral energy densities characterizing the important oceanic processes.

However an energy (or variance-preserving spectrum (Figure 7.44) is more useful for comparing the kinetic energy per unit volume of different processes. Clearly energy concentration in physical space is greatest for surface gravity waves with capillary

waves a close second.

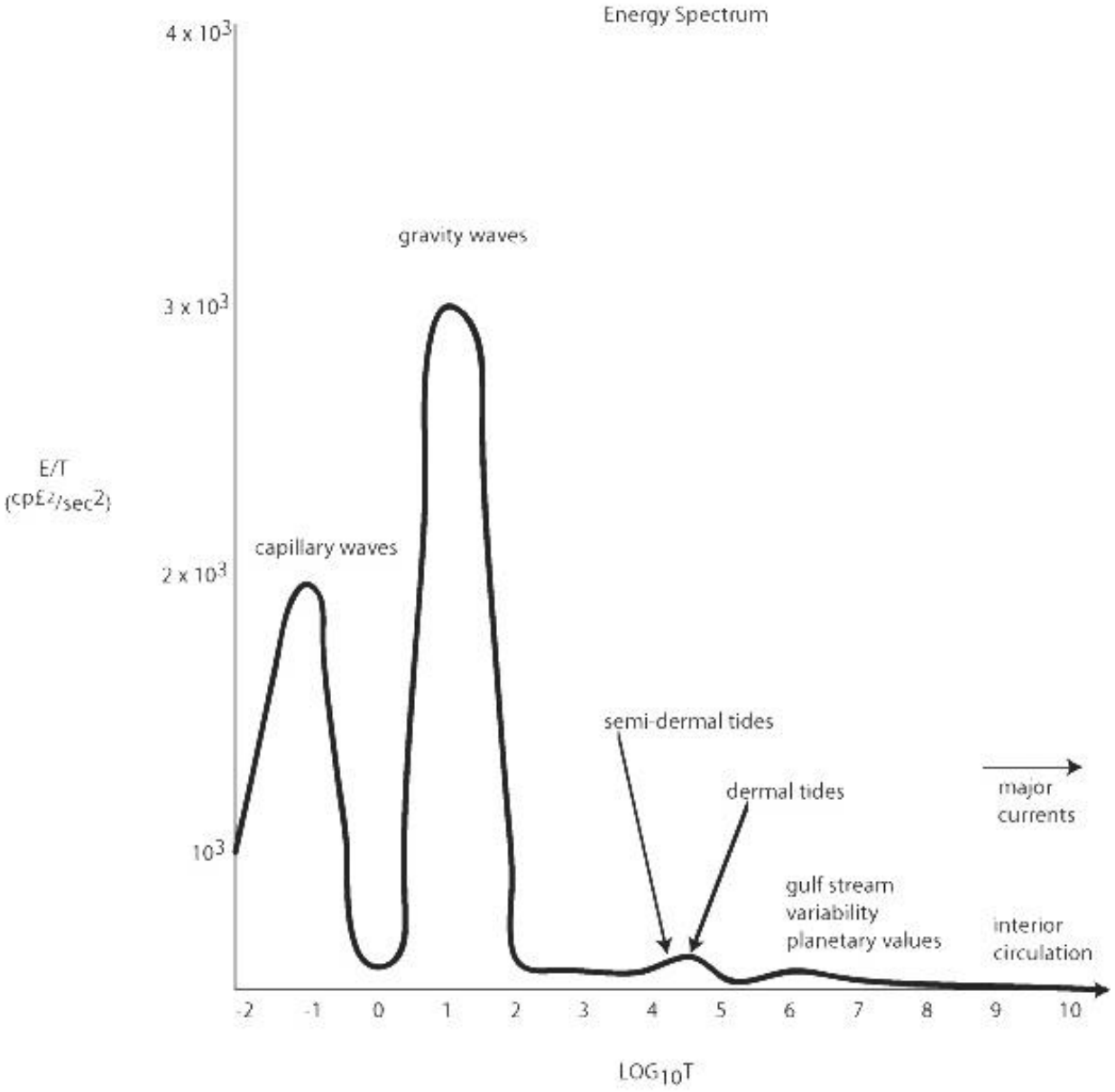

Figure 7. 44. Volume energy densities associated with the important oceanic processes.

Finally we summarize the dispersion characteristics of oceanic processes in terms of a wavelength wave period (Figure 7.45) of that set.

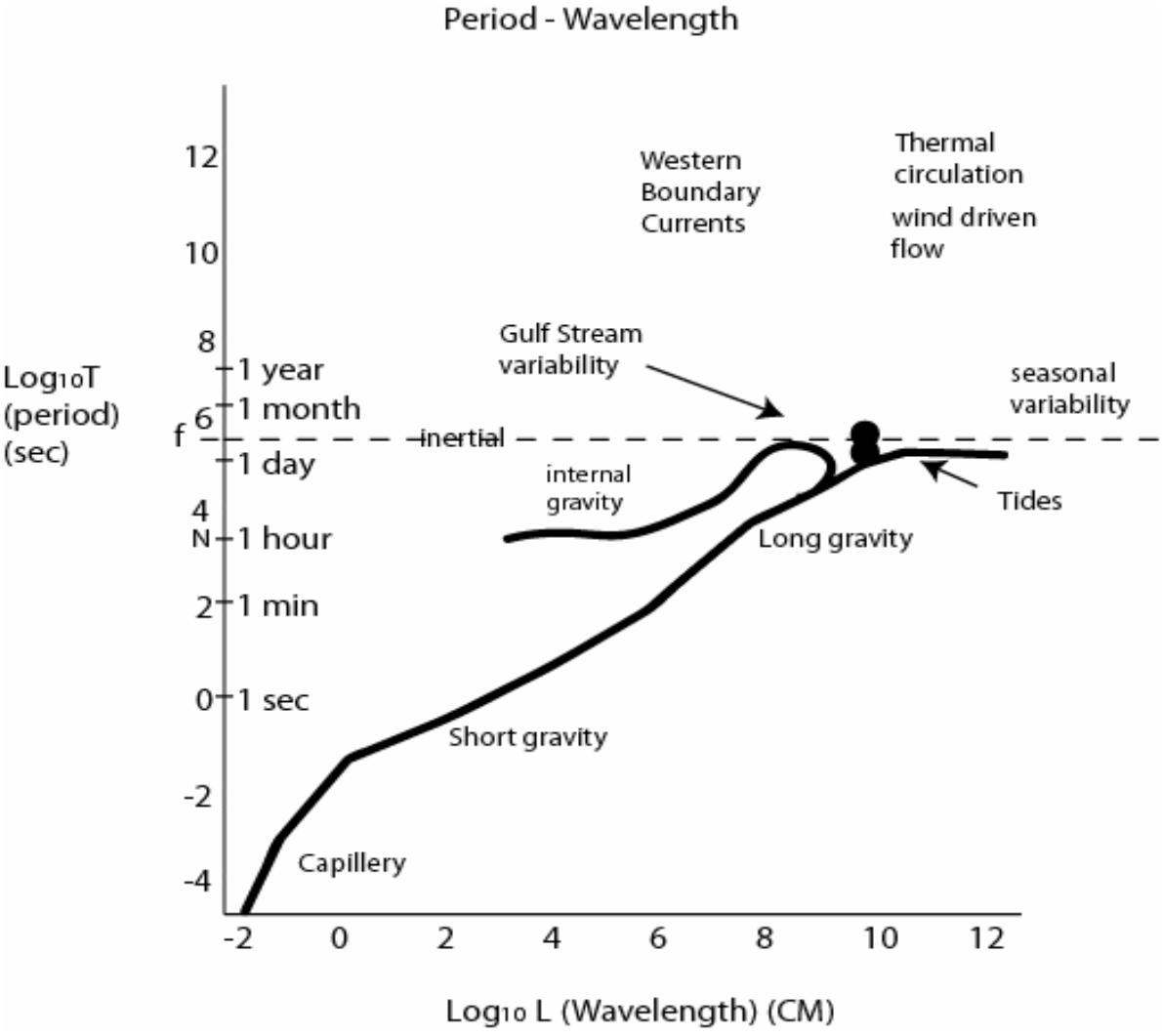

Figure 7. 45. Dispersion diagram for the principal oceanic processes.

PROBLEMS CHAPTER 7

Problem 7.1 Testing Airy Wave Solutions

Show that the Airy wave solutions (page 8 in the main text) algebraically satisfy the equations for continuity and momentum, as well as the boundary conditions, i.e.

Boundary Conditions:

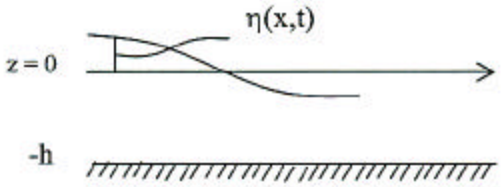

at $z = 0$ $\quad w = \frac{\partial \eta}{\partial t}$

$p = \rho g \eta$

at $z = -h$ $\quad w = 0$

Problem 7.2 Wave Kinematics

Show that the superposition (i.e. addition) of the following two waves

$$h_1 = (a/2)\cos[k_1 x - w_1 t)] \text{ and } h_2 = (a/2)\cos[k_2 x - w_2 t)]$$

where $k_2 > k_1$ and $w_2 > w_1$,

gives

$$h = a\cos[\frac{\Delta k}{2}(x - c_g t)]\cos[\bar{k}(x - \bar{c}t)] \quad ,$$

where $\Delta k = k_2 - k_1 \ll \bar{k}$, with $\bar{k} = \frac{k_1 + k_2}{2}$; $\quad \bar{c} = \frac{\bar{w}}{\bar{k}}$, $with \bar{w} = \frac{w_1 + w_2}{2}$. and

$c_g = \Delta w / \Delta k = (w_2 - w_1)/(k_2 - k_1)$, $with\ \Delta w = w_2 - w_1 << \bar{w}$

Problem 7.3 Wave Energetics

a) In general, *group velocity* of a wave is $Cg = \frac{dw}{dk}$. For Airy waves, with

$$w^2 = gk \tanh(kh) \ ,$$

show that

$$Cg = \frac{1}{2} C \left(1 + \frac{2kh}{\sinh 2kh}\right) \quad ,$$

where C = ? /k the phase velocity.

b) Given a wave of the form $h = a \cos(2p\, x/L)$, calculate the average kinetic energy per unit surface area , assuming Airy waves.. (Hint: assume $h = 0$ so the integral can be written

$$\overline{KE} = \frac{r}{2L} \int_0^L \int_{-h}^0 (u^2 + w^2)\, dx\, dz$$

c) How long would it take for energy associated with a deep water wave, with L = 100 m, to propagate 1000 km?

d) The deep water wave in part c) runs into shallow water near the coast and is observed to have a wave height H = 3 m in a water depth of 5 m. Compute its power at this depth. What would its amplitude a, wavelength L, and wave slope be in a water depth of 2 m? Are conditions for Airy Wave theory satisfied for the wave at this 2 m depth?

c) What is the power (in kilowatts) associated with 1 km alongshore segment of an H = 0.5m wave with a period of 5 seconds - a typical wave in the Gulf of Maine.

d) Assuming 20% efficiency in converting wave power to electrical power, compute how long a wave energy extraction facility would have to be in order to power New York City; with a 300 megawatt demand.

e) Speculate on the environmental impact of such a facility (assuming it could ever be constructed).

Problem 7.4 Long Waves

a) Given the sketch below

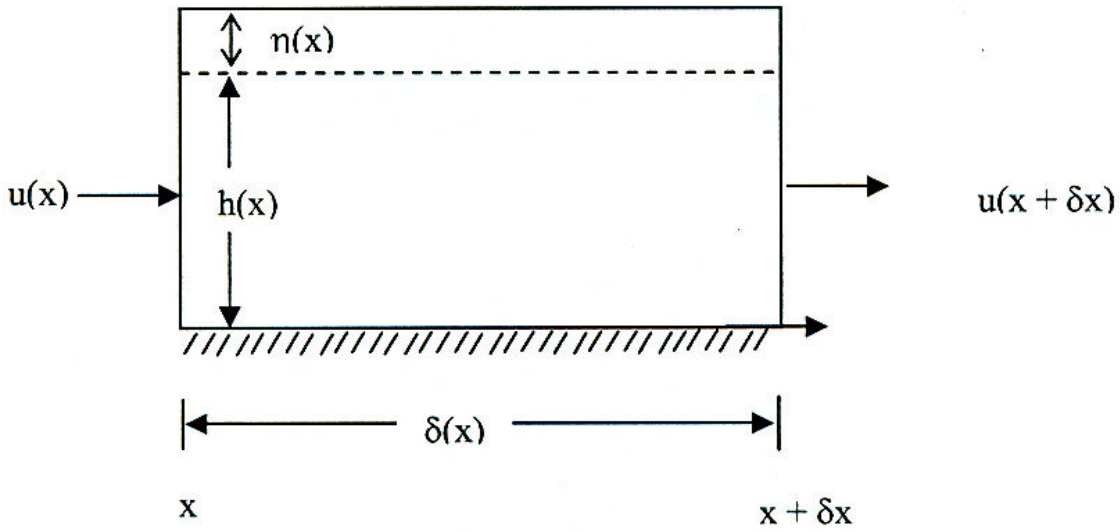

show that the one-dimensional continuity relation for shallow water waves for which the horizontal velocity is uniform with depth is:

$$\frac{\partial h}{\partial t} + \frac{\partial}{\partial x}\left[u(h + h)\right] = 0$$

and when $h / h << 1$ reduces to

$$\frac{\partial h}{\partial t} + h\frac{\partial u}{\partial x} = 0$$

b) Show that the following wave equation

$$\frac{\partial^2 h}{\partial t^2} - gh\frac{\partial^2 h}{\partial x^2} = 0$$

is satisfied by a long wave with the general solution

$$h = a\cos(kx \pm w t)$$

Problem 7.5 Basin Dynamics

a) The measured sea level at the inlet to the estuarine basin (triangle in figure a) reveals an oscillation with a period of 6 minutes superimposed on a tide record (figure a) .

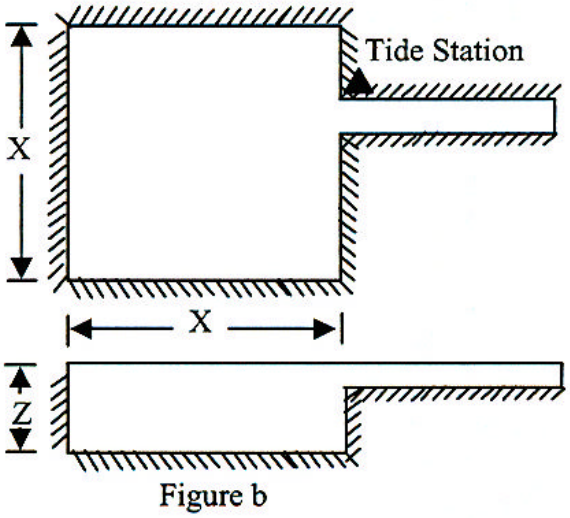

Figure b

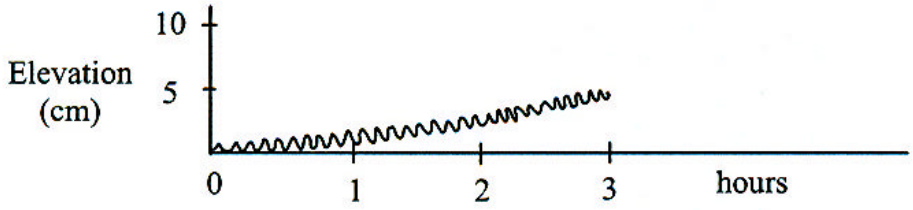

Figure a

a) Let us investigate the possibility that a basin standing wave might be responsible for the observed oscillation. Given that X = 2 km and the basin depth Z = 3m is constant; what is the allowed frequency of a first mode wave, i.e., one for which L = 2X? What is the wave period in minutes? What can you conclude about the observed oscillation?

b) What is the frequency of the M_2 tide?

c) What size must a basin (of depth equal to the one shown) be in order to allow a first mode standing wave with a frequency equal to that of the M_2 tide?

Problem 7.6 Propagation of Long Gravity Waves Onto the Continental Shelf

Consider the following model bathymetry below

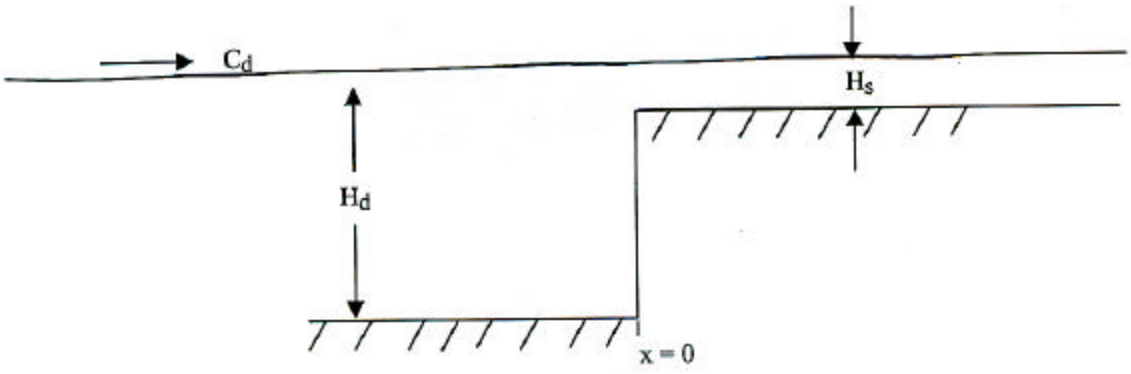

On the deep water side, the surface height field is composed of an incident wave and possible reflected waves according to

$$h_d = h_i \cos k(x - c_d t) + h_r \cos k(x + c_d t)$$

a) What is c_d?

On the shallow water side, there is a transmitted wave field on the shelf

$$h_s = h_t \cos k_s(x - c_s t).$$

At x = 0, the wave height must be is continuous according to

$$h_d(o, t) = h_s(o, t)$$

and the volume transports are equal

$$u_d(o, t) = u_s(o, t)$$

b) Evaluate both the reflection coefficient $R = \frac{h_r}{h_i}$ and the transmission coefficient $T = \frac{h_t}{h_i}$.

c) What is the energy reflection ratio $\frac{h_r^2}{h_i^2}$ and energy transmission ratio $\frac{h_t^2}{h_i^2}$.

d) Evaluate the reflection and transmission coefficients for a typical shelf where H_d = 4000 m and H_s = 100 m.

Problem 7.7 Channel Tides

Solve for free tidal waves in a channel as shown below

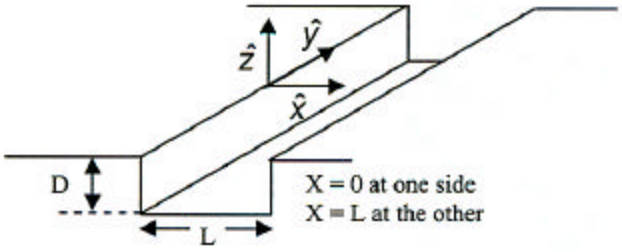

The equations of motion are (momentum and continuity)

$$\frac{\partial u}{\partial t} - fv + g\frac{\partial}{\partial x}h = 0$$

$$\frac{\partial v}{\partial t} + fu + g\frac{\partial}{\partial y}h = 0$$

$$\frac{\partial h}{\partial t} + \frac{\partial}{\partial x}(UD) + \frac{\partial}{\partial y}(VD) = 0$$

Assume ? of the form

$$h = h_{(x)}\,\mathrm{Exp}(i(\beta y - \omega t))$$

a. Solve the momentum equations for u and v to get

$$iu = \frac{g}{\omega^2 - f^2}\left[-f\beta + \omega\frac{\partial}{\partial x}\right]h$$

$$v = \frac{g}{\omega^2 - f^2}\left[\omega\beta - f\frac{\partial}{\partial x}\right]h$$

b. Then solve the continuity relationship to get a dispersion relationship of the form

$$gD(\alpha^2 - \beta^2) = \omega^2 - f^2$$

c. Take as boundary conditions that normal component of the velocity vanishes at the boundary, i.e., at x = 0 and x = L, i.e.

$$[-f\beta + \omega\frac{\partial}{\partial x}]h = 0$$

Get two cases for real and imaginary a, identify them, and i). solve for a and ß in both cases, ii). solve for c = ? /k in both cases.

Problem 7.8 Wave Force Balances

Oscillatory motion occurs when there is a restoring force acting on a displaced "particle", (generally proportional to the displacement). Describe the restoring force for such of these types of waves:

Inertial waves
Long surface gravity
Short surface gravity
Tides
Internal waves
Capillary waves

Indicate on a ? versus k plot where each of these waves might be found. (What are the range of wave numbers and angular frequencies for each?)

Problem 7.9 Short Wave Reflection

Suppose you have deep water gravity waves impinging on the side of the ship. What does the pattern of waves look like?

Let the ship be a wall at x = 0

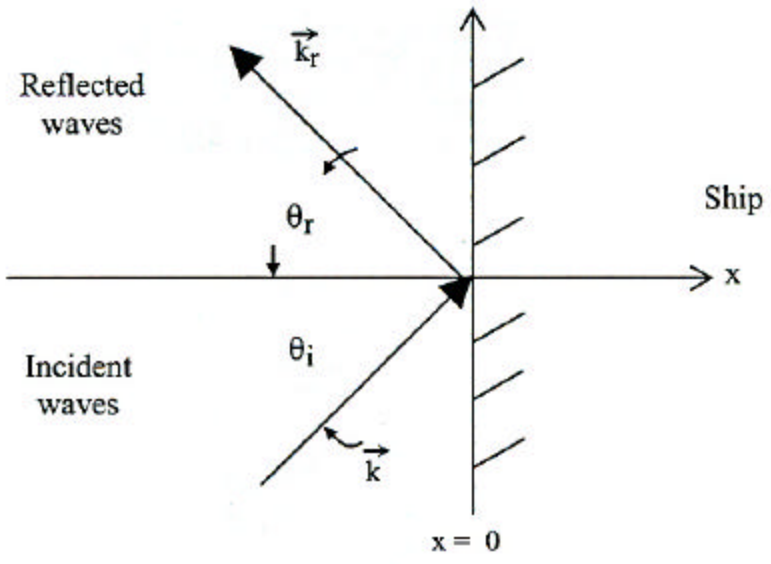

The surface height field will be the sum of incident and reflected waves according to

$$h = h_i \cos(kx + \ell y - w t) + h_r \cos(-k_r x + \ell_r y - w_r t)$$

.

a) What are w, u(x,y,z,t), v(x,y,z,t)?

b) Evaluate w_r, ℓ_r, h_r, and k_r for the condition of no flow through the side of the ship or u(x = 0, y, z, t) = 0

c) Describe the outgoing wave.

Hint: Use $w^2 = g[k^2 + \ell^2]^{1/2}$

and

$$p = -\rho gz + \rho g h_i \cos(kx + \ell y - w t)\, e^{\sqrt{k^2+\ell^2}\, z} + \rho g h_r \cos(-k_r + \ell_r y - w_r t)\, e^{\sqrt{k_r^2+\ell^2}\, z}$$

Problem 7.10 Surface Gravity Waves

Given a mean depths of 13 m for Narragansett Bay and 200m for the Gulf of Maine, estimate the wavelength, period and speed for the:

- Shortest shallow water (or "long") wave
- Longest deep water (or "short") wave

that propagate in both locations.

Problem 7.11 Tsunamis

An earthquake of the coast of Peru creates a wave for which L >> 4km. Estimate how long it takes for this wave to reach Japan.

